

NILU: OR 24/2003
REFERENCE: N-100159
DATE: JUNE 2003
ISBN: 82-425-1444-5

The Oslofjord POP Model v. 1.0

A Fugacity-Based Non-Steady State Non-Equilibrium Multimedia Fate and Transport Model

**Knut Breivik, Birger Bjerkg, Frank Wania, Jan
Magnusson, Aud Helland and Jozef M. Pacyna**

NILU: OR 24/2003
REFERANSE: N-100159
DATO: JUNE 2003
ISBN: 82-425-1444-5

The Oslofjord POP Model v. 1.0

A Fugacity-Based Non-Steady State Non-Equilibrium Multimedia Fate and Transport Model

Knut Breivik¹⁾, Birger Bjerkgeng²⁾, Frank Wania³⁾, Jan Magnusson²⁾, Aud Helland²⁾ and
Jozef M. Pacyna¹⁾



1)
Norwegian Institute for Air Research
Postboks 100, N-2027 Kjeller, Norway



2)
Norwegian Institute for Water Research
Postboks 173 Kjelsås, N-0411 Oslo, Norway



3)
University of Toronto at Scarborough,
Department of Physical and Environmental
Sciences, 1265 Military Trail, Scarborough,
ON, Canada M1C 1A4

Contents

	Page
Contents	1
Summary in Norwegian	3
Summary in English	5
1 Introduction	7
2 Description of environmental characteristics in the model	8
2.1 Compartmentalisation of the Oslofjord.....	8
2.2 Water mass balance	10
2.3 Seasonally variable environmental input parameters.....	11
2.4 Other environmental input parameters	12
2.4.1 Additional parameters describing dimensions	14
2.4.2 Particle concentrations	14
2.4.3 Content of organic matter and organic carbon on particles.....	14
2.4.4 Volume fractions and bulk densities	15
3 Description of chemical fate in the Oslofjord POP Model	17
3.1 Overview	17
3.2 Phase partitioning and Z-values	18
3.2.1 Physical-chemical properties of PCBs and environmental half-lives	18
3.2.2 Z-values	19
3.3 D-values describing transformation and transport	20
3.3.1 Description of air-seawater exchange	23
3.3.2 Description of seawater-sediment exchange	25
3.4 Chemical emissions, advective inflow and boundary conditions	27
3.4.1 Direct emissions to the aquatic environment	27
3.4.2 Advective inflow	27
3.4.3 Boundary conditions.....	27
3.5 Mass balance equations	28
4 References	30
Appendix 1 Glossary	33
Chemical Properties	36
Appendix 2 Water fluxes determined using the NIVA Fjord Model [<i>In Norwegian</i>]	39

Summary in Norwegian

Denne rapporten beskriver i detalj en såkalt fugasitetsbasert multimedia modell som er utviklet for å forstå og forutsi transport og omsetningsforhold for organiske miljøgifter i Oslofjorden. Modellen som er beskrevet er utviklet som del av forskningsprosjektet "Utvikling og evaluering av en modell-strategi for organiske miljøgifter i belastede fjordområder – en studie av PCB i Oslofjorden" finansiert av forskningsrådet (NFR, prosjektnummer 1405320/720). I grove trekk trenger modellen tre hovedtyper data for å beskrive fordeling, transport og levetid til organiske miljøgifter i fjorden. Den første typen informasjon er lokalitetsspesifikke data som gjenspeiler forholdene i Oslofjorden. Her har prosjektet dratt nytte av tidligere studier, særlig fysiske transportforhold og andre kartlegginger av miljøgiftbelastningen i Oslofjorden. For det annet krever modellen informasjon om fysikalsk-kjemiske parametre og levetider i miljøet, eksemplifisert her for PCB. Videre krever modellen beregninger på historiske tilførsler av PCB fra atmosfære, elver og direkte utslipp til sjøvann. Modellen vil bli tilgjengelig etter evaluering, og vil kunne installeres på de fleste PC'er av nyere dato. Modellen kan relativt enkelt modifiseres til å simulere oppførselen av andre miljøgifter i Oslofjorden.

Summary in English

This report describes in detail the development and parameterisation of the Oslofjord POP Model – a fugacity based mass balance model developed to understand and predict the fate of POPs in the Oslofjord, Norway. The model has been developed as part of a research project, entitled “Development and evaluation of a model strategy for POPs in contaminated fjord areas - a case study for PCBs in the Oslofjord” (NFR-project No. 140530/720). The model calculates the environmental distribution, transport and fate of POPs, based on information about environmental characteristics, physical-chemical properties and half-lives as well as historical emissions and advective inflows. After evaluation, the model – developed using Microsoft Visual Basic - will be available free of charge from NILU. It may be installed and run on any recent PC without the need for extra software requirements.

The Oslofjord POP Model v. 1.0

A Fugacity-Based Non-Steady State Non-Equilibrium Multimedia Fate and Transport Model

Acknowledgements

The Norwegian Research Council (NFR) is gratefully acknowledged for funding this project (Project No. 140530/720). We would also like to thank Hans Olav Hygen (Norwegian Meteorological Institute) for providing meteorological data and Jens Skei (NIVA) for his valuable input to this project in its early stages.

1 Introduction

On the Norwegian mainland, much of the environmental concern with respect to the occurrence of certain Persistent Organic Pollutants (POPs) at elevated levels, are due to local contamination, caused by historical and current releases. Specifically, high concentrations of POPs in many contaminated fjord areas are considered serious local environmental problems. In this project, the primary objective has been to increase the quantitative understanding concerning the local environmental distribution and fate of POPs by developing, applying and evaluating a model strategy for such pollutants in a contaminated fjord area. The ultimate goal by carrying out such activities is to elaborate and evaluate an operational tool for decision makers to assess the likely long-term impact of POP pollution to this particular fjord-system. A first and necessary step is to test it for a group of POPs of environmental concern at a location for which monitoring data are available for evaluation.

Oslofjorden was selected as the area of investigation because:

- (1) It has been, is and still will be under significant pressure from fluxes of various pollutants at potential harmful levels, entering this coastal environment (*i.e. vulnerability*)
- (2) It has a very important socio-economical and recreational value for the large population living in the area (*i.e. benefit of undertaking further studies*).
- (3) It is among the most studied and well-characterised environmental systems in Norway (*i.e. parameter availability*).

The Polychlorinated Biphenyls (PCBs) were selected as the compounds to be studied because:

- (1) PCBs are the main cause to the restrictions on consumption of fish and mussels in 13 (of a total of 27) areas in the Norwegian coastal zone.

- (2) High levels of PCB in cod liver suggest that PCB still is being cycled in the ecosystem. As a consequence the health authorities have recommended that cod liver from the inner Oslofjord (*north of Drøbak*) should not be consumed due to a concern for potential negative health impacts (*i.e. environmental relevance*).
- (3) PCBs are considered as ideal “model” POPs because individual congeners exhibit a wide range of properties (*and thus are expected to show differences in the environmental behaviour, fate and bioaccumulation*).
- (4) Useful information on the environmental concentrations of PCBs in this fjord is available from past studies (*i.e. data availability*), facilitating the model evaluation (“*validation*”).

A multimedia modelling approach was furthermore selected because PCBs are recognised as pollutants with a “multimedia” feature. That is, they are known to partition extensively between environmental phases, e.g. undergoing reversible deposition or being “leached” from sediments (e.g. Larsson, 1985) and capable to volatilise from aquatic surfaces (e.g. Jeremiason et al. 1994). Furthermore, a dynamic modelling approach was selected as it is recognised that the environmental levels of PCBs in the fjord today may in part be caused by historical emissions, reflecting the environmental lifetime of these pollutants.

In this report, we describe the development, parameterisation and model equations of the Oslofjord POP Model. The model presented may be classified as a non-steady state non-equilibrium multimedia fate and transport model (Level IV), designed to simulate the long-term environmental response due to changes in emissions. The current version of the Oslofjord POP model may be relatively easily be modified to simulate the fate of other POPs and related organic chemicals.

2 Description of environmental characteristics in the model

2.1 Compartmentalisation of the Oslofjord

As indicated, one of the key reasons for selecting the Oslofjord as a case study, is that it is well characterised with respect to its environmental characteristics (*see e.g. Baalsrud and Magnusson, 2002 for a general overview*). This greatly facilitates the compartmentalisation and parameterisation of the model with respect to the environmental parameters that are needed as input.

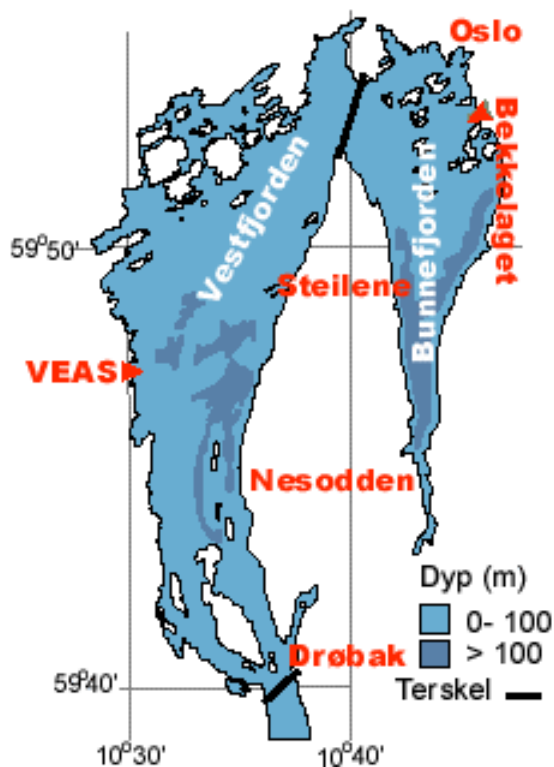


Figure 1. Map of the inner part of the Oslofjord. Light blue colour indicate a water depth from 0 to 100 meters, while dark blue indicate a depth of more than 100 meters.

As for most aquatic models of a similar type, the air-water interface and the river mouths constitute the system boundaries in this model. Therefore, riverine inflow concentrations and atmospheric concentrations over the aquatic compartments are model boundary conditions that need to be supplied by the user. In addition, the innermost part of the Oslofjord is connected to the outermost part of the Oslofjord as defined by the narrow and shallow strait at Drøbak (maximum depth of ~20 m). The Oslofjord may be characterised as a semi-enclosed water body.

In geographical terms, two major sub-basins are easily identified which are separately described in the Oslofjord POP Model. The eastern sub-basin is Bunnfjorden, which is separated from Vestfjorden through a wide strait, approximately 50 meters deep.

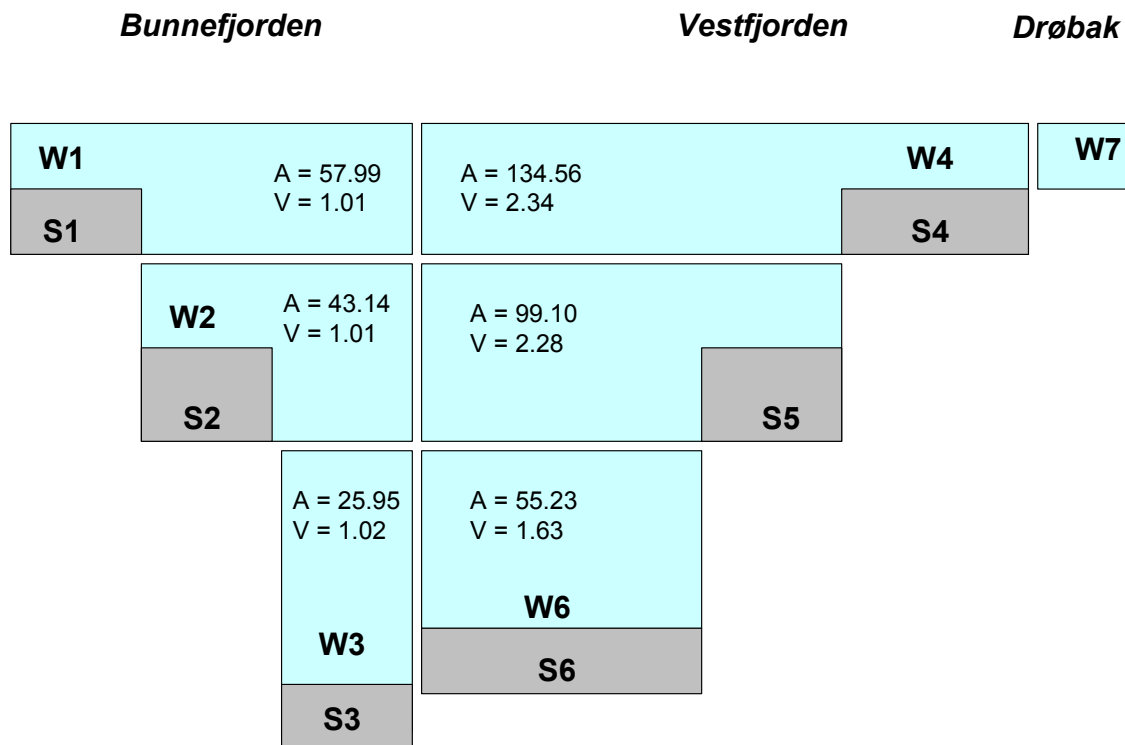


Figure 2: Compartmentalisation of the Oslofjord, showing surface area of the water compartments (A in km^2) and water volumes (V in km^3).

In order to resemble the key features of these two aquatic sub-basins in terms of water movement, a vertical subdivision of the two aquatic sub-units in the POP Model was implemented. As a necessary minimum, it was agreed to divide each sub-basin into three vertical segments in order to resemble and quantify the long-term transport behaviour of water masses (See 2.2). These horizontal layers are the upper layer (0-20 m), the middle layer (20-50m) and the bottom layer (50 m and below). The final compartmentalisation of the Oslofjord is given in Figure 2. The physical dimensions in terms of surface areas of the compartments and water volumes were taken from Munthe-Kaas (1967) – see also 2.4.1 and Table 1. As can be seen from Figure 2, the six aquatic compartments are further underlain by sediment layers, which are in contact with seawater. The two upper seawater layers are additionally in contact with the atmosphere. In addition, fresh water inflow is allowed to these two segments. The following indices are used here and in the remaining parts of the report to describe the various compartments and environmental phases; A = Atmosphere, Q = Aerosols, F = Fresh Water, W = Sea Water, S = Sediment, R = Re-suspended sediment solids.

2.2 Water mass balance

A consistent steady-state water mass balance was constructed in order to describe the main features of water transport in the fjord. The corresponding parameterisation of the physical transport of water masses - reflecting the compartmentalisation of the fjord (Figure 2) - were mainly derived from output from the NIVA Fjord Model (Bjerkeng, 1994). The NIVA Fjord Model has a high vertical resolution of the water column and a detailed description of density/pressure-driven water exchange between layers and basins. It also has a

detailed temporal resolution of physical processes, down to a scale of hours, and describes diurnal, seasonal and inter-annual variations.

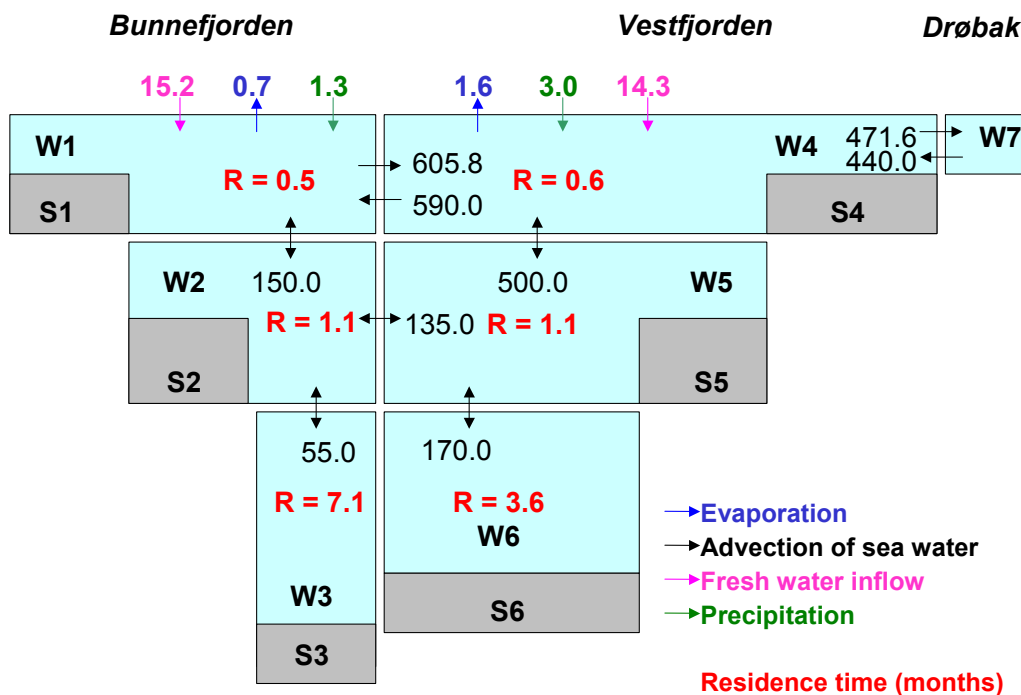


Figure 3: Long-term average water balance for the Oslofjord. Water fluxes are presented in m^3/sec and residence times are given in months.

A detailed analysis with the NIVA Fjord Model was undertaken in order to come up with representative figures for the exchange of water between the aquatic compartments as shown in Figure 3. In order to obtain representative long-term averages, the calculated values represent simulations over a period of 14 years. Similarly, water evaporation fluxes in $m^3 sec^{-1}$ from Bunnefjorden and Vestfjorden were also derived on the basis of output from the NIVA Fjord Model. A report describing the elaboration of these parameters is included as Appendix 2 to this report [In Norwegian].

The precipitation fluxes derived also reflect long-term averages, based on data supplied by the Norwegian Meteorological Institute (Station Fornebu, 1961-1990). Furthermore, the bulk riverine inflows to the two sub-basins were estimated based on information provided by local authorities and agencies (Oslo vann og avløpsetaten, Bærum kommune, Næringsmiddeltilsynet). Finally, net outward fluxes of water masses through the fjord (from W1 to W4 and from W4 to W7) were derived from the other water fluxes.

2.3 Seasonally variable environmental input parameters

A special emphasis within this project has been to achieve an increased understanding about the climatically - and thus seasonally dependent - partitioning and fate of PCBs under relevant Nordic climatic conditions. In contrast to the radionuclides, the environmental lifetime of PCBs and related compounds is strongly affected by the site-specific climatic and environmental characteristics (e.g. Webster et al. 1998; Mackay, 2001). Therefore, environmental partitioning processes and reaction rates are described using seasonally and spatially variable

temperatures as input (section 3.2 and 3.3). Furthermore, seasonally variable wind speeds over the seawater surface are used as input to estimate mass transfer coefficients to calculate air-water exchange of POPs (section 3.3 and Table 7). The long-term monthly average temperatures in air (T_A) are based on meteorological data from Fornebu from 1961 to 1990, while the long-term average monthly wind speeds was obtained, based on measured monthly averages from 1957 to 1998 from the same meteorological station (Norwegian Meteorological Institute). The temperature in fresh water is assumed to adapt the same monthly average temperature as air, except that the fresh water temperatures do not drop below 0 °C during winter time.

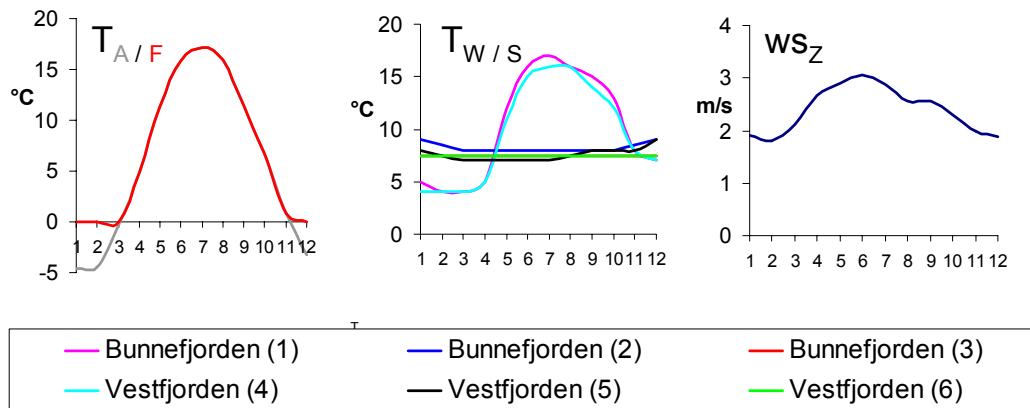


Figure 4: Seasonally variable environmental input parameters. Shown are the temperatures (in °C) in air (T_A) fresh water (T_F), seawater compartments (T_W), sediment compartments (T_S) and wind speed (ws_Z) in m/s. With the current parameterisation, $T_F = T_A$, and $T_S = T_W$.

Seasonally variable temperatures of the six seawater compartments (T_W) were derived from information presented by Magnusson et al (2000; 2001). Finally, the temperatures of the six sediment compartments (T_S) are assumed to adapt to the same temperatures as the corresponding seawater compartments. These seasonally variable parameters, converted into daily values using linear interpolation in the model, are shown in Figure 4.

2.4 Other environmental input parameters

The model also requires a number of other environmental input parameters to be specified that are all assumed fixed in time (Table 1). Ideally, these environmental parameters should reflect long-term average values and be representative of the entire compartments of interest. However, due to reasonable practical and economical reasons, measured data are generally too limited to fulfil these strict criteria.

Table 1: Environmental input parameters. Values in italics are estimated values.

Abbr.	Parameter	Atmosphere						Notes
C_Q	Air particle concentration [$\mu\text{g m}^{-3}$]	10						[A]
vOC_Q	Volume fraction OC on aerosols [v/v]	0.1						[B]
		Fresh water						
		Bunnefjorden			Vestfjorden			
C_{FP}	Particle concentration in fresh water [mg/L]	13.5			7.8			[C]
wOM_F	Weight frac. OM fresh water part. [w/w]	0.3			0.46			[C]
		Sea Water and Sediment Compartments						
		1	2	3	4	5	6	
C_{WP}	Seawater particle concentration [mg/L]	3.6	3.0	5.1	3	3	3	[D]
wOM_W	Weight fraction OM sea water particles [w/w]	0.4	0.4	0.4	0.4	0.4	0.4	[E]
wOC_S	Weight fraction OC sediment solids [w/w]	0.039	0.045	0.044	0.043	0.038	0.028	[F]
wOC_R	Weight fraction OC re-suspended sed. [w/w]	0.2	0.2	0.2	0.2	0.2	0.2	[G]
v_S	Volume fraction bulk solids in sediment [v/v]	0.14	0.14	0.14	0.14	0.14	0.14	[H]
H_S	Mean active sediment depth [m]	0.05	0.05	0.05	0.05	0.05	0.05	[E]
A_W	Surface area of seawater compartments [m^2]	Figure 2						
A_S	Surface area of sed. compartments [m^2]	$A_{W1} - A_{W2}$	$A_{W2} - A_{W3}$	A_{W3}	$A_{W4} - A_{W5}$	$A_{W5} - A_{W6}$	A_{W6}	
V_W	Volume of seawater compartments [m^3]	Figure 2						
V_S	Volume of sediment compartments [m^3]	Calculated as $A_S \cdot H_S$ for each sediment compartment						

[A] Typical concentration in the area - Leiv Håvard Slørdal, NILU (pers. comm.). [B] Wania and Daly, 2000. [C] Based on data from 8 major rivers in 2000 and 2001 [D] Based on data supplied by NIVA or *estimated*. [E] Assumed values (see text) [F] Sediment surface samples (0-2 cm, n=100). After Konieczny et al. (1994), $n = 10, 20, 16, 15, 16, 23$, respectively. [G] Assumed equivalent to the seawater particles OCs. [H] Based on data for 6 dated sediment cores (Konieczny et al. 1994; DHI, 2002).

This implies that several parameters may be criticised for lacking sound scientific empirical basis. Still, subjective judgements with respect to the available information have been unavoidable in order to come up with some of these input parameters, presented here and in the following. In order to achieve a certain transparency and to facilitate a replacement of some of these parameter values (if more reliable data may become available in the future), we have therefore chosen to document in some detail how the various input parameters were derived.

2.4.1 Additional parameters describing dimensions

As shown in the lower parts of Table 1, a volume of the accessible sediment layer is calculated by multiplying the sediment surface area (A_S) with a mean active sediment depth (H_S). It is clearly difficult to provide an unambiguous definition of these accessible sediment layers in terms of depth. As pointed out by Mackay (2001), it may be misleading to assume that sediment layer below about 5 cm is not accessible, albeit most of the activity of the burrowing organisms may be assumed to occur in this layer. Still, we have chosen to define the active sediment layer here as the upper 5 centimetres in all sediment compartments (see also 3.3.2).

2.4.2 Particle concentrations

PCBs and other POPs tend to associate or sorb to the organic carbon (OC) of particles. Therefore, the particle concentrations in various media are important inputs to the model (Table 1). Specifically, each of the environmental media addressed in the model require input information about the bulk particulate content (aerosols, suspended solids in water, sediments solids and re-suspended sediments).

The particulate concentration given in **air** (C_O) has been suggested as a typical concentration, based on measurements in the area (Leiv Håvard Slørdal, NILU). Concentrations of bulk particles in **fresh water** (C_{FP}) are based on monitoring data from eight major rivers draining into the fjord, while concentrations of bulk particles in **seawater** (C_{WP}) are based on data from Bunnefjorden (Aud Helland, NIVA) or assumed values in the case of Vestfjorden in the absence of empirical data.

The concentration of particles in **sediment** is described by the volume fraction of solids in sediments (vS). This term should reflect the depth of the defined active sediment. This parameter is available from dated sediment core studies at six stations in the fjord (Konicny et al. 1994; DHI, 1992). As expected, this parameter is generally showing an increase with sediment depth as water becomes “squeezed out” at greater sediment depths. For these six stations, vS were found to vary between 0.05 and 0.30 within the upper 5 centimetres. Because the data are few and limited to a limited area within the model domain, we have chosen to apply the average volume fraction of sediment solids from 0 to 5 centimetres ($vS \approx 0.16$) for all sediment compartments with no consideration to potential spatial differences (Table 1).

2.4.3 Content of organic matter and organic carbon on particles

The particles in various environmental compartments are all assumed to consist of defined fractions of **organic matter (OM)** and **mineral matter (MM)**. Sorption of hydrophobic contaminants is mainly expected to occur to the **organic carbon (OC)** of the organic matter (OM) on these particles. It is assumed in the following that all particles contain equal amounts of OM and OC (Mackay et al. 2001). In order to estimate the environmental partitioning

between the dissolved or gaseous phase and the sorbed phase (OC on particles), additional information on the OM content or OC content of these particles needs therefore to be supplied as input to the model. For particles in fresh water, seawater, sediments as well as re-suspended sediments, a weight fraction (w/w) of OM or OC on particles is provided (wOM_F , wOM_W , wOC_S and wOC_R). The choice of using both OM and OC as descriptors, are simply based on the availability of measurement data and their reported units.

For inflowing **fresh water particles**, wOM_F are based on measured values from the eight major rivers that have been monitored.

The weight fractions of OM on **seawater particles** (wOM_W) were estimated, considering (i) the reported values of wOM_F , (ii) information about concentrations of cell carbon in the fjord (Magnusson et al. 2001;2001) and (iii) concentrations of bulk water particles (C_{WP}). The presented estimates of wOM_W yields figures that are more or less equivalent to the generic values suggested by Mackay (2001).

Konieczny et al (1994) measured the content of TOC in surface sediment (0-2cm) at 100 locations in the Oslofjord. In addition, six sediment cores were taken down to a depth of 20 centimetres (*not the same as those that were dated*). Here, we assume TOC to be equal to OC on these sediment solids. It was expected that the weight fraction of organic carbon on **sediment solids** (wOC_S) was decreasing with depth (*due to digestion and degradation with increasing depth*), and that only the six sediment cores could be considered representative of the defined active sediment depth. Surprisingly, the TOC content were *on average* found to remain stable in these six cores, down to both 5 and 10 centimetres. Since it was not possible to discern a decreasing trend in wOC_S with depth from these measurements, we have chosen to base the estimates of wOC_S from the set of 100 surface samples (0-2 centimetres) to represent the active sediment depth (0-5 centimetres). These 100 samples were assigned to the respective sediment compartment of interest, and an average value was calculated for each of these (Table 1).

Finally, the organic carbon contents of **re-suspended sediment solids** (wOC_R) are assumed equivalent to the OC content of seawater particles ($wOC_R = 50\%$ of wOM_W).

2.4.4 Volume fractions and bulk densities

The model further requires that the volume fractions of organic carbon on particles are calculated in order to estimate Z-values of particles (Table 4). Similarly, bulk densities needs to be derived in order to calculate concentrations on a weight-by-weight basis. For these calculations, the mineral matter density (ρ_{MM}) is assumed to be to 2400 kg m^{-3} and the organic matter density (ρ_{OM}) is assumed equal to an organic carbon density (ρ_{OC}) of 1000 kg m^{-3} .

The **volume fractions (vOC_X) of organic carbon on particles** may be calculated as:

$$vOC_X = \frac{1}{2} \cdot \left\{ \frac{(wOM_X / \rho_{OC})}{[(wOM_X / \rho_{OC}) + [(1-wOM_X) / \rho_{MM}]]} \right\} \quad [\text{Eq. 1}]$$

or

$$vOC_X = \frac{(wOC_X / \rho_{OC})}{([2 \cdot wOC_X / \rho_{OC}] + [(1-(2 \cdot wOC_X)) / \rho_{MM}])} \quad [\text{Eq. 2}]$$

Here, subscript X may refer to F (Fresh water particles – Eq.1), W (Seawater particles – Eq.1), S (Sediment solids – Eq.2) or R (Re-suspended sediment solids – Eq.2).

For air particles, the volume fraction of organic carbon on particles (vOC_Q) is provided as direct input to the model (Wania and Daly, 2000).

The **bulk densities of particles** are deduced in the model from information about the volume fractions of organic carbon and the densities of organic carbon as well as mineral matter:

$$\rho_{XP} = 2 \cdot vOC_X \cdot \rho_{OC} + (1 - (2 \cdot vOC_X)) \cdot \rho_{MM} \quad [\text{Eq. 3}]$$

Here subscript X may refer to F,W,S,R or Q.

Finally, in order to calculate a bulk phase Z-value (see Table 4), it is a need to calculate the **volume fractions of (bulk) solids** in air, fresh water, seawater and sediments (vX). For sediments, the volume fraction of sediment solids is provided as direct input (Table 1), while it is calculated for fresh water, seawater and air particles. For air the volume fraction of air particles is calculated as:

$$vQ = C_Q \cdot 10^{-9} \cdot \rho_Q \quad [\text{Eq. 4}]$$

For fresh water particles ($X=F$) and seawater particles ($X=W$), the corresponding equation is:

$$vX = C_{XP} / 1000 \cdot \rho_{XP} \quad [\text{Eq. 5}]$$

3 Description of chemical fate in the Oslofjord POP Model

3.1 Overview

The Oslofjord POP model is a so-called multimedia fate and transport model, building upon the fugacity approach (Mackay, 1979; 2001). That is, the contaminant mass balance equations of individual environmental media are calculated with respect to fugacities (with unit of pressure). The core structure is similar to the QWASI-model (Mackay et al. 1983). However, this model consists of six similar segments, each sharing several similarities to the original core QWASI-model. Still, the Oslofjord POP model is (unlike QWASI) a non-steady state model, enabling the evaluation of environmental response to changes in emissions (Level IV). This is considered useful in this particular context, as a significant proportion of the PCBs that are found in the fjord today are assumed to be due to historical releases.

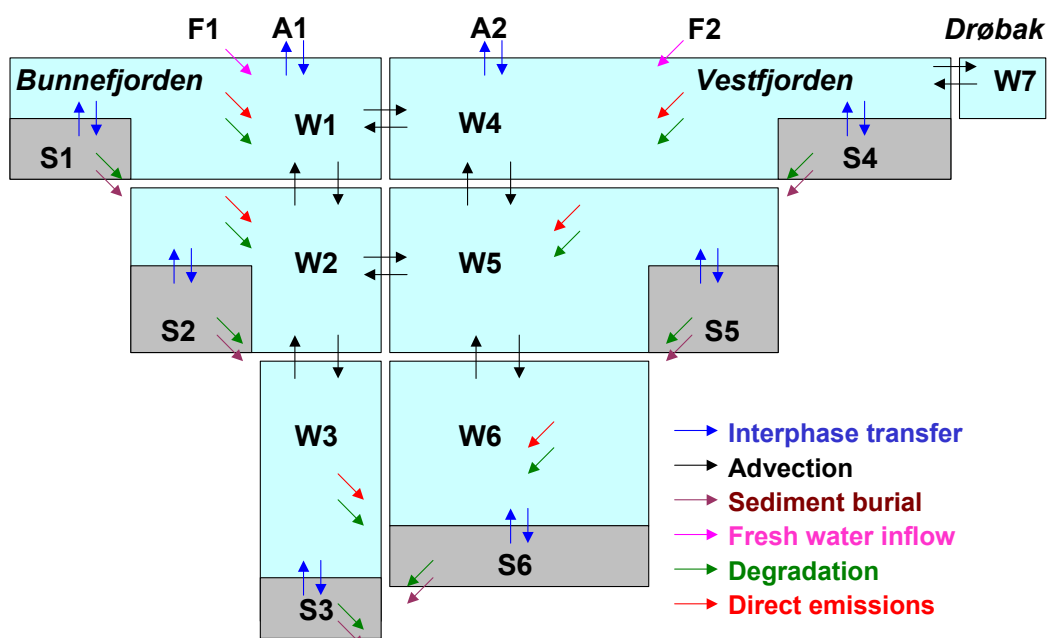


Figure 5: Bulk contaminant fate processes included in the Oslofjord POP Model.

The Oslofjord POP model also builds significantly upon the more comprehensive POPCYCLING-Baltic model (Wania et al. 2000). In particular, the treatment of transport and transformation is similar to the aquatic sub-models of the POPCYCLING-Baltic model, and the mass balance equations are solved in a similar fashion.

An outline of the various model compartments and bulk processes included in the Oslo POP Model is presented in Figure 5.

3.2 Phase partitioning and Z-values

3.2.1 *Physical-chemical properties of PCBs and environmental half-lives*

Phase partitioning in the Oslofjord POP model is expressed based on double logarithmic correlations between the environmental partitioning coefficients and a “well-known” partition coefficient (i.e. the equilibrium partition coefficients between octanol and water (K_{OW}), octanol and air (K_{OA}) and air and water (K_{AW})). The model requires that two of these are specified, and the third may then be deduced from the other two. Furthermore, in order to estimate the temperature dependencies of the well-known partition coefficients, the model requires the corresponding energies of phase transfer to be specified (ΔU_{OW} , ΔU_{OA} , ΔU_{AW}). Similarly, two out of three energies of phase transfer needs to be specified.

The parameter values for selected PCBs were collected from a recent study by Li et al (In Press). This particular data set of physical-chemical properties is considered superior to past compilations, as Li et al have presented an internally consistent set of physical-chemical properties that are based upon on all experimental evidence published so far. Environmental half-lives of the selected PCBs in sea water and sediments were based on the compilation by Sinkkonen and Paasivirta (2000) as quoted by Wania and Daly (2002), and converted to half-lives at 25 °C. Finally, a uniform activation energy of 30 kJ mol⁻¹ was assumed for degradation in water and sediments (Wania and Daly, 2002).

These parameter values are listed, along with the molecular mass of the selected PCBs, in Table 2. The temperature dependence of these well-known partition coefficients (K_{OW} , K_{AW} and K_{OA}) is deduced, based on the ideal gas constant and the consecutive expressions given in Table 3. In these expressions, T_x refers to the temporally and spatially variable temperature of the phase of interest (in Kelvin). An equilibrium partition coefficient between particulate organic carbon and water (K_{OC}) is furthermore calculated, based on the empirical relationship presented by Seth et al (1999). The Henrys law constant may be calculated by multiplying the ideal gas constant with the specific phase temperature and the air-water partitioning coefficient.

Table 2. Molecular weight (MW), partition coefficients (K) at 25 °C [A], energies of phase transfer (ΔU) [A], degradation half-lives in water and sediments at 25 °C (HL) [B] and activation energies (Ea) [C].

	#28	#52	#101	#118	#138	#153	#180
MW (g/mol)	257.44	291.99	326.43	326.43	360.9	360.9	395.3
log K_{OW} (-)	5.66	5.91	6.33	6.69	7.21	6.87	7.16
log K_{OA} (-)	7.85	8.22	8.73	9.36	9.66	9.44	10.16
ΔU_{OW} (kJ mol ⁻¹)	-26.3	-27.3	-23.8	-28.5	-25.0	-31.1	-29.1
ΔU_{OA} (kJ mol ⁻¹)	-78.5	-81.4	-83.5	-89.0	-86.3	-93.9	-92.8
HL _W (hours)	5500	10000	31000	46000	46000	55000	55000
HL _S (hours)	17000	55000	55000	100000	100000	170000	170000
Ea (kJ mol ⁻¹)	30	30	30	30	30	30	30

[A] Li et al (*in press*), [B] Based on information in Wania and Daly (2002) and references therein or *estimated*, [C] Wania and Daly (2002).

Table 3: Ideal gas constant (R) and temperature dependence of key partitioning properties and degradation rates [Eqs. 6-13].

Parameter	Constant or expression	Notes
R	8.314 J K ⁻¹ mol ⁻¹	
Log $K_{OW}(T_x)$	Log $K_{OW}(25^\circ\text{C}) + (\Delta U_{OW} / 2.303 \cdot R) \cdot (1/298.15 - 1/T_x)$	[A]
Log $K_{AW}(T_x)$	Log $K_{AW}(25^\circ\text{C}) + (\Delta U_{AW} / 2.303 \cdot R) \cdot (1/298.15 - 1/T_x)$	[A]
Log $K_{OA}(T_x)$	Log $K_{OA}(25^\circ\text{C}) + (\Delta U_{OA} / 2.303 \cdot R) \cdot (1/298.15 - 1/T_x)$	[A]
$K_{POC}(T_x)$	0.35 · $K_{OW}(T_x)$	[B]
$H(T_x)$	R · T_x · $K_{AW}(T_x)$	[A]
$k_{RW}(T_W)$	$k_{RW}(25^\circ\text{C}) \cdot e^{\{Ea / R \cdot [1/298.15 - 1/T_W]\}}$	[A]
$k_{RS}(T_S)$	$k_{RS}(25^\circ\text{C}) \cdot e^{\{Ea / R \cdot [1/298.15 - 1/T_S]\}}$	[A]

[A] Wania et al. 2000. [B] Seth et al. 1999.

Finally, the degradation in water and sediment is assumed to follow first order kinetics. In this case, the relationship between a first order degradation rate constant (k_R) and an environmental half-life (HL) is given by $HL = \ln(2) / k_R$. Based on the Arrhenius equation, the first order degradation rate constants for bulk seawater (k_{RS}) and bulk sediments (k_{RW}) are expressed as functions variable temperatures of seawater and sediments (T_W and T_S , respectively).

3.2.2 Z-values

Environmental concentrations are usually reported as amount per weight or volume, but when comparing concentrations in various compartments, no obvious information about the flux of chemicals can easily be obtained. Fugacity is an entity, with units of pressure, which can be utilised to estimate the movement of chemicals between environmental compartments (Mackay, 1979; Mackay, 1991).

Table 4: Z-values in $\text{mol m}^{-1} \text{Pa}^{-1}$ at compartmental temperatures [Eqs. 14-29].

Par.	Description	Expression	Note
ZA	Pure air	$1 / R \cdot T_A$	[A]
ZQ _A	Atmospheric particles	$ZA(T_A) \cdot K_{OA}(T_A) \cdot vOC_Q \cdot \rho_Q / \rho_{OCT}$	[B]
ZW _X	Pure water		[A]
	X = R: Rain water	$1 / H(T_A)$	
	X = W: Sea water	$1 / H(T_W)$	
	X = F: Fresh water	$1 / H(T_F)$	
	X = S: Sediment water	$1 / H(T_S)$	
ZOC _X	Organic Carbon		[A]
	X = F: Fresh water	$ZW_F(T_F) \cdot K_{OC}(T_F) \cdot \rho_{OC} / 1000$	
	X = W: Sea water	$ZW_W(T_W) \cdot K_{OC}(T_W) \cdot \rho_{OC} / 1000$	
	X = S: Sediment	$ZW_S(T_S) \cdot K_{OC}(T_S) \cdot \rho_{OC} / 1000$	
ZP _X	Bulk Particles		[A]
	X = W: Seawater	$vOC_W \cdot ZOC_W(T_W)$	
	X = F: Fresh water	$vOC_F \cdot ZOC_F(T_F)$	
	X = S: Sediment part.	$vOC_S \cdot ZOC_S(T_S)$	
	X = R: Resusp. Sed.	$vOC_R \cdot ZOC_W(T_W)$	
BZ _W	Bulk sea water	$(1-vW) \cdot ZW_W(T_W) + vW \cdot ZP_W(T_W)$	[A]
BZ _F	Bulk fresh water	$(1-vF) \cdot ZW_F(T_F) + vF \cdot ZP_F(T_F)$	[A]
BZ _S	Bulk sediment	$(1-vS) \cdot ZW_S(T_S) + vS \cdot ZP_S(T_S)$	[A]

[A] Based on Mackay 2001 [B] Wania and Daly 2002.

When concentrations of adjacent compartments are converted to fugacity, the fugacity level can be compared and the net movement of chemical can be predicted. The chemical will tend to escape from the media with the high fugacity level to the media with low fugacity level. When the fugacity or “escaping tendency” of a given chemical in adjacent compartments is equal, the chemical is in equilibrium.

Z-values are proportionality constants that relate fugacity to concentrations. Z-values can further be regarded as “half” partition coefficients and are calculated in the Oslofjord POP Model as given in Table 4.

3.3 D-values describing transformation and transport

Advective and diffusive transport processes, as well as transformation processes, are described in the model with the help of D-values (D , $\text{mol h}^{-1} \text{Pa}^{-1}$), using the nomenclature of Mackay (2001). Advective transport D-values are products of a flow rate, called G-values (G , $\text{m}^3 \text{h}^{-1}$) and Z-values (Z , $\text{mol m}^{-1} \text{Pa}^{-1}$). A D-value, multiplied with the source fugacity (f_x), results in a process rate (mol/h).

Transformation D-values are expressed as the sum of $V \cdot k_R \cdot Z$. In the latter equation, k_R is the first order rate constant (k_R , h^{-1}), V is the compartment volume (V , m^3) and the Z-value corresponds to the (bulk) compartment for which the reaction occurs. The term 3600, which is included in several of these equations

(Table 5), is a factor to convert advective flow rates from $\text{m}^3 \text{sec}^{-1}$ to $\text{m}^3 \text{h}^{-1}$, using the parameter values as shown in Figure 3.

The D-values used to calculate transport and transformation processes are summarised in Table 5. It is immediately apparent that these D-values are dependent on a number of other model parameters that are yet to be defined, notably some G-values and some additional transport parameters that are utilised to describe air-seawater exchange and seawater-sediment exchange. These additional parameters are listed in Table 6 (G-values) and Table 7 (additional transport parameters).

In the following, we outline how these were derived.

Table 5: Transport and transformation process descriptions (D-values) in $\text{mol h}^{-1} \text{Pa}^{-1}$ [Eqs. 30-49].

Par.	Process	Source f	Expression
DQ _A	Dry particle deposition	f _A	GQ _A · ZQ _A
DM _A	Pure rain water dissolution	f _A	GM _A · ZW _A
DC _A	Wet particle deposition	f _A	GC _A · ZQ _A
DV	Air-sea water diffusion (volatilisation and absorption)	f _A / f _W	1 / [1/(mtc _A · A _W · Z _A) + 1/(mtc _W · A _W · ZW _W)]
DB _A	Total atmospheric deposition	f _A	DQ _A + DM _A + DC _A + DV
DR _W	Sea water reaction (bulk)	f _W	BZ _W · V _W · k _{RW}
DW _{YZ}	(Pure) sea water advection – W(Y) to W(Z)	f _W	G _{YZ} · 3600 · ZW _W
DP _{YZ}	Sea water particle advection - W(Y) to W(Z)	f _W	G _{YZ} · 3600 · v _W · ZP _W
D _{YZ}	Bulk sea water advection - W(Y) to W(Z)	f _W	DW _{XY} + DP _{XY}
DD _W	Sediment deposition	f _W	GD _W · ZP _W
DT	Overall seawater-to-sediment diffusion (both directions)	f _W / f _S	1 / {(1/DT _{BW}) + (1/[DT _{BS} + DT _{BB}])}
DT _{BW}	Water-side molecular diffusion through the boundary layer		A _S · k _{SW} · ZW _W (T _W)
DT _{BS}	Sediment-side molecular diffusion through water-filled pores		A _S · (B _{eff} / [0.39 · H _S]) · ZW _S (T _S)
DT _{BB}	Sediment-side biodiffusivity		A _S · (B _{bio} / [0.39 · H _S]) · ZP _S (T _S)
DB _S	Sediment burial	f _S	GB _S · ZP _S
DR _S	Sediment re-suspension	f _S	GR _S · ZP _R
DS _R	Sediment reaction (bulk)	f _S	BZ _S · V _S · k _{RS}
DI _F	(Pure) fresh water advection	f _F	G _{FW} · 3600 · ZW _F
DX _F	Fresh water particle advection	f _F	G _{FW} · 3600 · v _F · ZP _F
DB _F	Bulk fresh water advection	f _F	DI _F + DX _F
D _{XYXZ}	Net exchange D-value from compartment X(Y) to X(Z)		

3.3.1 Description of air-seawater exchange

PCBs may be deposited to the sea surface by dry and wet particle deposition, rain dissolution and through gaseous absorption (diffusion). Similarly, PCBs may re-volatilise from the sea surface by diffusion.

The D-values used to derive dry and wet particle deposition and rain dissolution are obtained by multiplying the corresponding G- and Z-values as given at the top of Table 5. The equation used to quantify the flux of dry particles to the sea surface (G_{QA}) is given in Table 6 for which the dry deposition velocity (dd_Q) were adapted from Wania et al (2000) - see Table 7. Next, the rain rate (rr_A - Table 7) is converted into a flow rate (G_{MA}) in $m^3 h^{-1}$, utilising a conversion factor (8760000) and taking into account the areas of the sea surface (A_W). Wet particle deposition is described in the form of a G-value as the product of the rain “flux” (G_{MA} - Table 6), a scavenging ratio ($SCVG_A$ - see Table 7) and by the volume fraction of bulk particles in air (vQ - Equation 4).

Table 6: Additional G-values as included in Table 5 (all values in m^3/h) [Eqs. 50-55].

Abbr.	Description	Expression
G_{QA}	Dry particle deposition	$A_W \cdot dd_Q \cdot vQ$
G_{MA}	Pure rain water deposition	$(rr_A \cdot A_W) / 8760000$
G_{CA}	Wet particle deposition	$G_{MA} \cdot SCVG_A \cdot vQ$
GD_W	Sediment deposition	$(UDP_S \cdot vS \cdot A_S) / (24 \cdot 365 \cdot 1000)$
GB_S	Sediment burial	$(UBS_S \cdot vS \cdot A_S) / (24 \cdot 365 \cdot 1000)$
GR_S	Sediment re-suspension	$(URS_S \cdot vS \cdot A_S) / (24 \cdot 365 \cdot 1000)$

Volatilisation and absorption are described by the two-resistance concept, originally applied to air-seawater exchange by Liss and Slater (1974) for which the reciprocal D-values add to give a reciprocal total (Mackay, 2001), i.e. $1/DV = 1/D1 + 1/D2$. Here D1 describes the resistance on the air side ($mtc_A \cdot A_W \cdot Z_A$) and D2 describes the resistance on the water side ($mtc_W \cdot A_W \cdot ZW_W$). The mass transfer coefficients (mtc_A and mtc_W) used to describe DV are furthermore calculated as functions of the long-term average wind speeds at a reference height of 10 m (Table 7), based on an approach developed by Mackay and Yuen (1983).

Table 7: Additional transport parameters and expressions as included in Table 5 [Eqs 56-61].

Abbr.	Parameter	Atmosphere						Notes
dd _Q	Dry particle dep. velocity - [m/h]	1.03						[A]
rr _A	Annual precipitation - [mm/yr]	714						[B]
SCVG _A	Scavenging ratio - [-]	68000						[A]
z	Wind measurement height - [masl]	10						[B]
ws _z	Wind speed at z m.a.s.l. [m/s]	Figure 4						[B]
ws ₁₀	Wind speed, 10 m.a.s.l. [m/s]	$ws_z / \{[(\ln z + 8.1) / 10.4]\}$						[C]
mtc _A	Air-side MTC - [m/h]	$0.065 \cdot [6.1 + (0.63 \cdot ws_{10})]^{0.5} \cdot ws_{10} \cdot 36$						[D]
mtc _W	Water-side MTC - [m/h]	$0.000175 \cdot [6.1 + (0.63 \cdot ws_{10})]^{0.5} \cdot ws_{10} \cdot 36$						[D]
		Sea Water and Sediment Compartments						
		1	2	3	4	5	6	
UDB _S	Sediment Burial [mm year ⁻¹]	5.5	4.5	3.5	3	2	1	[E]
fPB _S	Fract. of Deposition being Buried [-]	0.6	0.75	0.9	0.6	0.75	0.9	[F]
UDP _S	Sediment Deposition [mm year ⁻¹]	UDB _S / fPB _S						
URS _S	Re-suspension [mm year ⁻¹]	UDP _S - UDB _S						
k _{SW}	Overall MTC (water-side) [m h ⁻¹]	0.01	0.01	0.01	0.01	0.01	0.01	[F]
B _W	Mol. diffusivity in water [m ² h ⁻¹]	4·10 ⁻⁶	4·10 ⁻⁶	4·10 ⁻⁶	4·10 ⁻⁶	4·10 ⁻⁶	4·10 ⁻⁶	[F]
B _{eff}	Effective diffusivity in water [m ² h ⁻¹]	$B_W \cdot (1-vS)^{1.5}$						[F]
B _{bio}	Biodiffusivity in sediments [m ² h ⁻¹]	1·10 ⁻¹⁰	1·10 ⁻¹⁰	1·10 ⁻¹²	1·10 ⁻¹⁰	1·10 ⁻¹⁰	1·10 ⁻¹⁰	[G]
	log mean diffusion path length	0.39	0.39	0.39	0.39	0.39	0.39	[H]

[A] Wania et al. 2000 [B] Norwegian Meteorological Institute [C] Mackay and Yuen (1983) as quoted by Schwarzenbach et al. 1993. [D] Mackay and Yuen (1983) as quoted by Wania et al. 2000. [E] After Konieczny et al (1994) [F] Based on Mackay (2001). [G] Adapted from Wania et al. 2000, but assumed to be of limited significance at S3 because of anoxic conditions. [H] Adapted from Wania et al. 2000.

Specifically, it converts the measured monthly wind speeds (ws_z in $m s^{-1}$) into a reference height at 10 meters above sea level (ws_{10} in $m s^{-1}$) using the algorithm in Table 7. Two mass transfer coefficients are calculated on the basis of monthly variable wind speeds, ws_{10} . One is the stagnant atmospheric boundary layer mass transfer coefficient (mtc_A in $m h^{-1}$) and the second is the stagnant water layer mass transfer coefficient (mtc_W in $m h^{-1}$). Additional transport parameters utilised to describe atmospheric deposition (dry particle deposition velocity and scavenging ratio) in Table 7 were adopted from Wania et al. 2000.

As can be seen from Table 5, the same expression applies to describe diffusion in both directions, except that the source fugacity is different when the process rates are deduced as DV times f_X . Finally, a total D-value for transport from the atmosphere to the seawater surface is deduced as $DQ_A + DM_A + DC_A + DV$ (Table 5).

3.3.2 Description of seawater-sediment exchange

There are two processes that may bring PCBs from the seawater compartments to the underlying sediments. These are sediment deposition (DD_W) and diffusion (DT). At the same time, there are two processes that may act in the opposite direction, namely sediment re-suspension (DR_S) and diffusion (DT). Furthermore there are two “permanent” loss processes from the sediment compartments included in the model. The first one is (bulk) sediment reaction (DS_R) and the second is sediment burial (DB_S).

Sediment, when deposited may either be re-suspended or – eventually – become buried (i.e. below the active sediment layer). The sediment burial rate is thus equal to the net sediment accumulation rate. Thus, the total deposition rate of sediments is equal to the sum of the rates describing sediment burial and re-suspension.

Konieczny et al (1994) presented sediment accumulation rates in the Oslofjord. Specifically, sediment accumulation rates were derived for the five dated sediment cores, and these findings were discussed in comparison with previous studies and other results presented in their report. Based on their assessment, they propose a suggested sediment accumulation rate of 4 to 5 $mm year^{-1}$ to be representative for Bunnefjorden, and a rate of about 2 $mm year^{-1}$ to be representative for Vestfjorden. These net deposition rates are thus equal to the **burial rates** in the model (expressed as UDB_S Table 7), as the depth of the active sediment layer is considered to be static in the model. Furthermore, as these net deposition rates or burial rates are expected to be generally higher in shallow areas than in the deeper parts of the fjord, the proposed values were adjusted to take this into account (Table 7).

The measurements of sediment **deposition** rates are clearly difficult, due to the presence of the reverse process of sediment **re-suspension**. Still, they are both considered as potentially important fate processes affecting the cycling of PCBs in the fjord. It was therefore considered important to make an attempt to simulate these processes to assess the potential relative importance of these, although no site-specific information was available.

As an initially attempt to simulate deposition and re-suspension, we assume here that the relative importance of these processes are equal to the generic values proposed in the generic Level III model by Mackay (2001). That is, it is being assumed that 75% of the sediment that are being deposited is eventually buried while 25% is re-suspended back into the water column. Again, these values were slightly adjusted to reflect a higher relative re-suspension rate in the shallow parts of the fjord and a correspondingly lower re-suspension rate in the deeper parts of the fjord. These preliminary estimates of sediment deposition (UDP_S) and sediment re-suspension (URS_S) are presented in Table 7.

The G-values (in $m^3 h^{-1}$) that are derived to describe sediment deposition (GD_W), burial (GB_S) and re-suspension (GR_S) have fairly similar expressions, listed in Table 6, and the corresponding D-values are listed in Table 7 as DD_W , DB_S and DR_S , respectively.

Diffusion between seawater and sediments are described using a similar overall approach as presented by Wania et al. (2000). Three different diffusive processes between seawater and sediment are considered, which may act in either direction. On the seawater side, there is a resistance to transfer through the stagnant boundary layer above the sediment surface. This process is described by a water-side stagnant boundary layer D-value (DT_{BW}) in $mol h^{-1} Pa^{-1}$. Secondly, there are two resistances described on the sediment side of the seawater sediment interface. One is describing the diffusion through water-filled pore spaces in the sediment (DT_{BS}) and the other is describing “bio-diffusivity” (DT_{BB}). The first D-value (DT_{BW}) acts in series to the two parallel resistances on the sediment side, DT_{BS} and DT_{BB} . A total D-value for water-sediment diffusion may therefore be expressed as (Table 5):

$$DT = 1 / \{ (1/DT_{BW}) + (1/[DT_{BS} + DT_{BB}]) \}$$

Diffusion through the stagnant **water boundary layer** is further described by (Mackay et al. 2001):

$$DT_{BW} = A_S \cdot k_{SW} \cdot ZW_W(T_W)$$

where A_S is the surface area of the sediment compartment (Table 1 in m^2), k_{SW} is a water-side mass transfer coefficient in $m h^{-1}$ (Table 7), and $ZW_W(T_W)$ is the Z-value for water at sea water temperatures (in the stagnant boundary layer on the water side) in $mol m^{-3} Pa^{-1}$ (Table 4).

DT_{BS} - or **molecular diffusion through the sediment pore spaces** - are expressed by:

$$DT_{BS} = A_S \cdot (B_{eff} / [0.39 \cdot H_S]) \cdot ZW_S(T_S)$$

Here, B_{eff} is the calculated effective diffusivity in sediment in $m^2 h^{-1}$, described in the equation above as $B_W \cdot (1-vS)^{1.5}$, where B_W is the molecular diffusivity in water in $m^2 h^{-1}$ and vS is the volume fraction of solids in sediment (Mackay, 2001). Furthermore, the parameters used to estimate DT_{BS} are 0.39 which is the log mean diffusion path length, H_S is the depth of the active sediment depth in meters, and ZW_S is the Z-value for water at sediment temperatures.

Finally, DT_{BB} - or **bio-diffusivity** - is expressed as

$$DT_{BB} = A_S \cdot (B_{bio} / [0.39 \cdot H_S]) \cdot ZP_S(T_S)$$

where B_{bio} is a bioturbation diffusivity in $m^2 h^{-1}$, and ZP_S is the Z-value for sediment solids at sediment temperatures.

The parameter values utilised for these calculations are listed in Table 7.

3.4 Chemical emissions, advective inflow and boundary conditions

3.4.1 Direct emissions to the aquatic environment

The model requires that direct emissions to the six aquatic compartments are specified for individual PCB congeners for a given reference year (in Kg/Year). Key sources of relevance are the sewer systems that discharge into the fjord system (Johansen and Samdal, 1995). In addition, a reference year for which the specified emission rates apply needs to be provided. Finally, the historical trend of these aquatic emissions is scaled based on a suggested predefined time-trend starting in 1930 (Breivik et al. 2002), which may be redefined by the user.

3.4.2 Advective inflow

As mentioned, chemicals may also be entering the model domain by fresh water inflow and by atmospheric deposition.

Fresh water inflow is simulated by specifying a representative concentration for the fresh water inflow to Bunnefjorden and Vestfjorden (in pg/L), which is multiplied by the fresh water inflow to these two fjord units. Atmospheric deposition is calculated by the model, based on measured concentrations of PCBs in the atmosphere (in pg/m^3). As for the emissions, a reference year for the defined concentrations in fresh water and atmosphere needs to be specified individually, corresponding to each concentration value. Finally, the long-term trend is simulated based on the suggested time-trend (which may be changed by the user).

3.4.3 Boundary conditions

Finally, PCBs may enter the model domain via seawater through Drøbak and into the upper aquatic compartment of Vestfjorden. The boundary conditions are simulated as a ratio, describing the concentration difference between W4 and seawater outside Drøbak and its change in time. This fraction and its temporal trend have to be specified by the user. A ratio higher than 1 means that the concentration is higher on the outside than on the inside, while a ratio of less than 1 implies that the concentration on the outside is less than the concentration on the inside. It should be noted that the Z-values of seawater outside the model domain and the upper water compartment at Vestfjorden are assumed having the same value (i.e. similar temperature, water particle concentration and organic carbon content). Only the flow rates (and thus D-values) are different (Figure 3 and Table 5).

3.5 Mass balance equations

The non-steady state mass balance equations can generally be expressed on the form (Wania et al. 2000):

$$\frac{dM(t)}{dt} = \frac{d[V(t) \cdot Z(t) \cdot f(t)]}{dt} = N_{in}(t) - D_T(t) \cdot f(t) \quad [\text{Eq. 62}]$$

$M(t)$	Amount of chemical in a compartment at time t in mol
$V(t)$	Volume of compartment at time t in m^3
$Z(t)$	Z-value of a compartment at time t in $\text{mol} / \text{m}^3 \cdot \text{Pa}$
$f(t)$	Fugacity in a compartment at time t in Pa
$N_{in}(t)$	Total input rate into a compartment at time t in mol/h
$D_T(t)$	D-value for total loss from a compartment at time t in $\text{mol} / \text{h} \cdot \text{Pa}$

For each of the twelve compartments, a non-steady state mass balance equation is solved at each user-defined time-step, dt (Table 8). In these equations, E stands for a direct emission rate in mol h^{-1} , D stands for a D-value in $\text{mol h}^{-1} \text{Pa}^{-1}$, and f stands for fugacity in Pa.

These equations are solved using a finite difference approximation (Wania et al. 2000):

$$\frac{d\{[V(t+dt) \cdot Z(t+dt) \cdot f(t+dt)] - [V(t) \cdot Z(t) \cdot f(t)]\}}{dt} = N_{in}(t) - D_T(t) \cdot f(t) \quad [\text{Eq. 63}]$$

However, the unsteady state solutions would require information about defined initial conditions. In the dynamic segmented QWASI model, the volume of each compartment is held constant, and the step-wise solution can be written as:

$$f(t+dt) = \{1 / Z(t+dt)\} \cdot \{[(dt / V(t)) \cdot (N_{in}(t) - D_T(t) \cdot f(t))] + Z(t) \cdot f(t)\} \quad [\text{Eq. 64}]$$

Table 8: Mass balance equations for seawater and sediment compartments.

Sea Water	[Equations 65-70]
W1	$dM_{W1}/dt = E_{W1} + D_{F1W1} \cdot f_{F1} + D_{A1W1} \cdot f_{A1} + D_{S1W1} \cdot f_{S1} + D_{W2W1} \cdot f_{W2} + D_{W4W1} \cdot f_{W4} - f_{W1} \cdot (D_{W1W2} + D_{W1W4} + D_{W1A1} + D_{W1S1} + D_{RW1})$
W2	$dM_{W2}/dt = E_{W2} + D_{S2W2} \cdot f_{S2} + D_{W1W2} \cdot f_{W1} + D_{W3W2} \cdot f_{W3} + D_{W5W2} \cdot f_{W5} - f_{W2} \cdot (D_{W2W1} + D_{W2W3} + D_{W2W5} + D_{W2S2} + D_{RW2})$
W3	$dM_{W3}/dt = E_{W3} + D_{S3W3} \cdot f_{S3} + D_{W2W3} \cdot f_{W2} - f_{W3} \cdot (D_{W3W2} + D_{W3S3} + D_{RW3})$
W4	$dM_{W4}/dt = E_{W4} + D_{F2W4} \cdot f_{F2} + D_{A2W4} \cdot f_{A2} + D_{S4W4} \cdot f_{S4} + D_{W5W4} \cdot f_{W5} + D_{W1W4} \cdot f_{W1} + D_{W7W4} \cdot f_{W7} - f_{W4} \cdot (D_{W4W1} + D_{W4W5} + D_{W4A2} + D_{W4S4} + D_{W4W7} + D_{RW4})$
W5	$dM_{W5}/dt = E_{W5} + D_{S5W5} \cdot f_{S5} + D_{W4W5} \cdot f_{W4} + D_{W6W5} \cdot f_{W6} + D_{W2W5} \cdot f_{W2} - f_{W5} \cdot (D_{W5W4} + D_{W5W6} + D_{W5W2} + D_{W5S5} + D_{RW5})$
W6	$dM_{W6}/dt = E_{W6} + D_{S6W6} \cdot f_{S6} + D_{W5W6} \cdot f_{W5} - f_{W6} \cdot (D_{W6W5} + D_{W6S6} + D_{RW6})$
Sediments	[Equations 71-76]
S1	$dM_{S1}/dt = D_{W1S1} \cdot f_{W1} - f_{S1} \cdot (D_{S1W1} + D_{RS1} + D_{BS1})$
S2	$dM_{S2}/dt = D_{W2S2} \cdot f_{W2} - f_{S2} \cdot (D_{S2W2} + D_{RS2} + D_{BS2})$
S3	$dM_{S3}/dt = D_{W3S3} \cdot f_{W3} - f_{S3} \cdot (D_{S3W3} + D_{RS3} + D_{BS3})$
S4	$dM_{S4}/dt = D_{W4S4} \cdot f_{W4} - f_{S4} \cdot (D_{S4W4} + D_{RS4} + D_{BS4})$
S5	$dM_{S5}/dt = D_{W5S5} \cdot f_{W5} - f_{S5} \cdot (D_{S5W5} + D_{RS5} + D_{BS5})$
S6	$dM_{S6}/dt = D_{W6S6} \cdot f_{W6} - f_{S6} \cdot (D_{S6W6} + D_{RS6} + D_{BS6})$

4 References

- Baalsrud, K. and Magnusson, J. (2002) Indre Oslofjord – natur og miljø. Oslo, Fagrådet for vann- og avløpsteknisk samarbeid i indre Oslofjord.
- Bjerkeng, B. (1994) Eutrofimodell for indre Oslofjord. Rapport 2: Faglig beskrivelse av innholdet i modellen. Oslo (NIVA Lnr 3113/94).
- Breivik, K., Sweetman, A., Pacyna, J.M. and Jones, K.C. (2002) Towards a global historical emission inventory for selected PCB congeners – a mass balance approach. *Sci. Total Environ.*, 290, 199-224.
- DHI (2002) ²¹⁰Pb-datering af en sedimentkerne fra Bunnefjorden, Norge. Hørsholm, DHI Institut for Vand og Miljø. (In Danish).
- Finizio, A., Mackay, D., Bidleman, T.F. and Harner, T. (1997) Octanol-air partition coefficients as a predictor of partitioning of semivolatile organic chemicals to aerosols. *Atmos. Environ.*, 31, 2289-2296.
- Jeremiason, J.D., Hornbuckle, K.C. and Eisenreich, S. J. (1994) PCBs in Lake Superior, 1978-1992. Decrease in water concentrations reflect loss by volatilization. *Environ. Sci. Technol.*, 28, 903-914.
- Konieczny, R.M., Berglund, L., Breivik, E.M., Kjellberg, F., Lauritzen, B.H., Tellefsen, T. and Villø, M. (1994) Miljøgiftundersøkelser i Indre Oslofjord. Delrapport 4: Miljøgifter i sedimenter. Oslo, Norsk institutt for vannforskning (Statlig program for forurensningsovervåking. Rapport 561/94).
- Larsson, P. (1985) Contaminated sediments of lakes and oceans act as sources of chlorinated hydrocarbons for release to water and atmosphere. *Nature*, 317, 347-349.
- Li, N., Wania, F., Lei, Y.D. and Daly, G.L. (2003) A comprehensive and critical compilation, evaluation and selection of physical chemical property data for selected polychlorinated biphenyls. *Journal of Chemical Engineering Data*. In Press.
- Liss, P.S. and Slater, P.G. (1974) Flux gases across the air-sea interface. *Nature*, 247, 181-184.
- Mackay, D., (1979) Finding fugacity feasible. *Environ. Sci. Technol.*, 13, 1218-1223.
- Mackay, D. (1983) A quantitative water, air, sediment interaction (QWASI) model for describing the fate of chemicals in lakes. *Chemosphere*, 12, 981-997.
- Mackay, D. and Yuen, A.T.K. (1983) Mass transfer coefficient correlations for volatilisation of organic solutes from water. *Environ. Sci. Technol.*, 17, 211-216.

- Mackay, D. (2001) Multimedia environmental models – the fugacity approach. 2nd ed. Boca Raton, Lewis Publishers.
- Magnusson, J., Johnsen, T., Gjørøæther, J., Lømsland, E.R. and Solli, A. (2000) Overvåking av forurensnings situasjonen i indre Oslofjord i 1999. Oslo, Norsk institutt for vannforskning (Statlig program for forurensningsovervåking. Rapport 798/00).
- Magnusson, J., Berge, J.A., Bjerkeng, B., Bokn, T., Gjørøæther, J., Johnsen, T., Lømsland, E.R., Schram, T.A. and Solli, A. (2001) Overvåking av forurensnings situasjonen i indre Oslofjord i 2000. Oslo, Norsk institutt for vannforskning (Statlig program for forurensningsovervåking. Rapport 825/01).
- Munthe-Kaas, H. (1967) Oslofjorden og dens forurensnings-problemer. Delrapport 15. Fjordens topografi. Oslo, Norsk institutt for vannforskning.
- Schwarzenbach, R.P., Gschwend, P.M. and Imboden, D.M. (1993) Environmental organic chemistry. New York, Wiley.
- Seth, R., Mackay, D. and Muncke, J. (1999) Estimating the organic carbon partition coefficient and its variability for hydrophobic chemicals. *Environ. Sci. Technol.*, 33, 2390-2394.
- Sinkkonen, S. and Paasivirta, J. (2000) Degradation half-life times of PCDDs, PCDFs and PCBs for environmental fate modelling. *Chemosphere*, 40, 943-949.
- Stene-Johansen, S. and Samdal, J.E. (1995) Miljøgifter in indre Oslofjord. Delrapport 5: Kartlegging av kilder. Oslo, Norsk institutt for vannforskning (Statlig program for forurensningsovervåking. Rapport 611/95).
- Wania, F., Persson, J., Di Guardo, A. and McLachlan, M.S. (2000) The POPCYCLING-Baltic Model. A non-steady state multicompartiment mass balance model of the fate of persistent organic pollutants in the Baltic Sea environment. Kjeller (NILU OR 10/2000).
- Wania, F. and Daly, G. (2002) Estimating the contribution of degradation in air and deposition to the deep sea to the global loss of PCBs. *Atmos. Environ.*, 36, 5581-5593.
- Webster, E., Mackay, D. and Wania, F. (1998) Evaluating environmental persistence. *Environ. Toxicol. Chem.*, 17, 2148-2158.

Appendix 1

Glossary

Environmental properties

Compartment Dimensions

A_X	Surface area of compartment in m^2 ($X=S,W$)
H_X	Average depth of compartment in m ($X=S,W$)
V_X	Volume of compartment in m^3 ($X=S,W$)

Volume fractions in m^3/m^3

v_F	Volume fraction of suspended solids in fresh water
v_W	Volume fraction of suspended solids in sea water
v_S	Volume fraction of solids in sediments
v_Q	Volume fraction of aerosols in air
v_{OC_Q}	Volume fraction of organic carbon (OC) on air particles
v_{OC_F}	Volume fraction of OC on suspended solids in fresh water
v_{OC_W}	Volume fraction of OC on suspended solids in sea water
v_{OC_R}	Volume fraction of OC on resuspended solids in sea water
v_{OC_S}	Volume fraction of OC on sediment solids

Weight fractions in kg/kg

w_{OM_F}	Weight fraction of OM on suspended solids in fresh water
w_{OM_W}	Weight fraction of OM on suspended solids in sea water
w_{OM_R}	Weight fraction of OM on resuspended solids in sea water
w_{OM_S}	Weight fraction of OM on sediment solids

C_{WP}	Concentration of dissolved solids in sea water in mg/L
C_{FP}	Concentration of dissolved solids in fresh water in mg/L
C_Q	Concentration of air particles in $\mu g/m^3$

ρ_{OC}	Density of organic carbon in g/m^3 ($=\rho_{OM}$)
ρ_{MM}	Density of mineral matter in g/m^3
ρ_{Oct}	Density of octanol in g/m^3
ρ_{XP}	Density of bulk particles in g/m^3 ($X = Q,F,W,R,S$)

T_A	Temperature in air in K
T_F	Temperature in fresh water in K
T_W	Temperature in sea water compartments in K
T_S	Temperature in sediment compartments in K

Transport parameters

$SCVG_A$	Particles scavenging ratio (dimensionless)
----------	--

Mass Transfer Coefficients in m/h

mtc_A	Air-side mass transfer coefficient over water in m/h
mtc_W	Water-side mass transfer coefficient in m/h
dd_Q	Air particle deposition velocity to sea water in m/h
B_W	Molecular diffusivity in water in m^2/h

B_{eff}	Effective molecular diffusivity in sediment pore water in m^2/h
B_{bio}	Biodiffusivity in sediment in m^2/h
WS_z	Wind speed at z meters above sea level
WS_{10}	Wind speed at 10 meters above sea level

Water advection rates

G_{YZ}	Sea water flow from W(Y) to W(Z) in m^3/sec
r_A	Precipitation rate in mm/year
G_{MA}	Precipitation rate in m^3/h
G_{FW}	Riverine inflow in m^3/sec

Particle advection rates

UDP_S	Sediment deposition rate in mm year^{-1}
UDB_S	Sediment burial rate in mm year^{-1}
URS_S	Sediment resuspension rate in mm year^{-1}
GD_W	Sediment deposition rate in m^3 / h
GB_S	Sediment burial rate in m^3 / h
GR_S	Sediment resuspension rate in m^3 / h
GQ_A	Dry particle deposition in m^3/h
GC_A	Wet particle deposition in m^3/h

Chemical Properties

R	Ideal gas constant in $\text{J} / \text{K} \cdot \text{mol}$
MW	Molecular weight in g/mol
K_{OW}	Octanol-water partition coefficient (dimensionless)
K_{OA}	Octanol-air partition coefficient (dimensionless)
K_{AW}	Air-water partition coefficient (dimensionless)
K_{POC}	Part. Organic Carbon-water partition coefficient (dim.less)
ΔU_{OW}	Energies of octanol-water phase transfer in J/mol
ΔU_{AW}	Energies of air-water phase transfer in J/mol
ΔU_{OA}	Energies of octanol-air phase transfer in J/mol
H	Henry's law constant in $\text{Pa} \cdot \text{mol} / \text{m}^3$
k_{RW}	Bulk reaction rate in water in h^{-1}
k_{RS}	Bulk reaction rate in sediment in h^{-1}
HL_W	Half-life in water in hours
HL_S	Half-life in sediment in hours
E_a	Activation energy of the reaction in J/mol
f	Fugacity of compartment in Pa

Z-values in $\text{mol} / (\text{m}^3 \cdot \text{Pa})$

ZA	Pure air
ZQ _A	Atmospheric particles
ZW	Pure water (A,W,F,S)
ZOC	Organic Carbon (W,F,S)
ZP	Bulk Particles (W,F,S,R)
BZ _X	Bulk phase Z-values (W,F,S)

D-values in mol / (h · Pa)

DQ _A	Dry particle deposition
DM _A	Pure rain water dissolution
DC _A	Wet particle deposition
DV	Air-sea water diffusion (absorption and volatilisation)
DB _A	Total atmospheric deposition
DR _W	Sea water reaction (bulk)
DW _{YZ}	(Pure) sea water advection – W(Y) to W(Z)
DP _{YZ}	Sea water particle advection – W(Y) to W(Z)
D _{YZ}	Bulk sea water advection - W(Y) to W(Z)
DD _W	Sediment deposition
DT	Overall seawater-to-sediment diffusion (both directions)
DT _{BW}	Water-side molecular diffusion through boundary layer
DT _{BS}	Sediment-side molecular diffusion through water-filled pores
DT _{BB}	Sediment-side biodiffusivity
DB _S	Sediment burial
DR _S	Sediment re-suspension
DS _R	Sediment reaction (bulk)
DI _F	(Pure) fresh water advection
DX _F	Fresh water particle advection
DB _F	Bulk fresh water advection
D _{XYXZ}	Net exchange D-value from compartment X(Y) to X(Z)

Appendix 2
Water fluxes determined using the NIVA Fjord
Model [*In Norwegian*]

1. Innledning

POP-modellen opererer med gjennomsnittskonsentrasjoner i de større volumene (0-20 m, 20-50 m og 50 m – bunn) og trenger tall for toveis vanntransporter over grenseflatene mellom volumene slik at en får riktigst mulig stofftransport mellom volumene når transportene opererer på gjennomsnittskonsentrasjoner innenfor hvert volum.

Opgaven er å beregne slik volumutveksling mellom volumene i POP-modellen ved hjelp av fjordmodellen, som har en mye finere vertikal inndeling av vannmassene. Umiddelbart kunne en tenke at det kunne gjøres direkte ved å hente ut transportene over de grenseflatene i fjordmodellen som tilsvarer grensene i POP-modellen, men det vil ikke bli riktig. Årsaken til det er at disse transportene bare berører direkte en liten del av POP-modellvolumene, og gir stofftransport ut fra konsentrasjonene i lagene omkring den aktuelle grenseflaten, og ikke ut fra gjennomsnittskonsentrasjonene i de større volumene. Det er den videre utvekslingen mellom fjordmodell-lagene innenfor hvert POP-volum som bestemmer virkningen på volumet som helhet.

For å få det til best mulig, utnyttes en mekanisme i fjordmodellen som beregner oppholdstider innenfor et antall definerte volumer. Dette beskrives nærmere nedenfor. Midlere oppholdstid over et slikt volum defineres da som den gjennomsnittlige 'alder' på vannet innenfor volumet, dvs. hvor lenge det vannet som ved et gitt tidspunkt finnes innenfor volumet i gjennomsnitt har oppholdt seg der. Denne størrelsen kan behandles som en konsentrasjon ($\text{tid} \cdot \text{volum} / \text{volumenhet}$), og de endringene en får pga. transport kan derfor tilsvare omtrent de endringer en kan få pga. av transport i andre konsentrasjoner. Dvs. at ved å regne seg tilbake fra oppholdstid til ekvivalent transport kan en prøve å få tall som gir omtrent riktig stofftransport anvendt på gjennomsnittskonsentrasjonen i de store volumene.

Presist kan det ikke bli, fordi det ville forutsette likedannede profiler for konsentrasjoner av forskjellige komponenter mellom forskjellige deler av de store volumene. For å kunne gi en riktig beskrivelse av forskjeller mellom store volumer, og av stofftransport mellom dem, kreves egentlig en volumoppdeling som er så fin at variasjonene innenfor hvert lag, som ikke kan beskrives annet enn helt grovt, er uvesentlig i forhold til de forskjellene mellom store volumer som en tar sikte på å løse opp.

Det er ikke mulig å sette opp en beregning som gir entydige transporttall som både representerer stofftransporter og gir volumkontinuitet innenfor en slik volumintegreert modellbeskrivelse. Det innses lett ved å tenke seg et tilfelle hvor en vil beskrive utveksling mellom to større volumer hvor det ene i realiteten er lagdelt, med store interne forskjeller, og det andre er effektivt blandet internt. Det kan da være effektiv utveksling mellom en liten del av det lagdelte volumet og hele det velblandede volumet, mens det meste av det lagdelte volumet er lite involvert. Den aktive delen av det lagdelte volumet kan igjen stå i intensiv kontakt med et tredje volum, og derved formidle stofftransport videre, uten at hele volumet berøres. Transporten fra det lagdelte til det velblandede volumet vil da bare i liten grad berøre gjennomsnittskonsentrasjonen i volumet, slik at den effektive vanntransporten den veien kan være svært forskjellig fra den reelle fysiske vanntransporten. Den andre veien, fra det velblandede volumet til det lagdelte volumet, vil effektiv transport være omtrent lik den fysiske transporten. De effektive transportene ville da ikke gi volumkontinuitet.

Nedenfor er det valgt å sette å opp et system av transporter som gir volumkontinuitet, og som gir oppholdstider som er har omtrent riktig størrelsesorden.

Kapittel 2 beskriver hvordan oppholdstid beregnes for et generelt tilfelle, og hvordan en i prinsippet kan regne seg tilbake til midlere tall for effektive transport inn i volumene.

Kapittel 3 beskriver hvordan fjordmodellen kan brukes til dette, og kapittel 3.3 hvordan avledede transporttall for hvert volum kan settes sammen til utvekslingstall mellom volumene.

2. Generelt om sammenheng oppholdstid – vannutveksling

2.1 Enkelt velblandet volum

Anta at vi har vannvolum, som kan variere over tid med volum $V(t)$. Volumet antas å være velblandet, dvs. at blandingstiden er mye kortere enn oppholdstiden.

Strømningene inn i og ut av volumet kan også variere over tid, de kalles $q_{inn}(t)$ og $q_{ut}(t)$. Hver av dem kan være satt sammen av flere adskilte strømmer. Gjennomsnittlig oppholdstid τ for vannet innenfor volumet til enhver tid har da en presis definisjon som den tid vannmolekylene i gjennomsnitt har oppholdt seg innenfor volumet. Utviklingen av oppholdstiden som funksjon av tid defineres av differensialligningen.

$$\frac{d(V\tau)}{dt} = V - q_{ut}\tau$$

Ved å bruke betingelsen om volumkontinuitet $(dV/dt) = q_{inn} - q_{ut}$ kan dette skrives

$$\frac{d\tau}{dt} = 1 - \frac{q_{inn}}{V}\tau \quad \text{eller} \quad q_{inn} = \frac{V}{\tau} \left(1 - \frac{d\tau}{dt} \right)$$

hvor alle symbolene q , V , τ står for størrelser som kan variere over tid.

Hvis en har beregnet hvordan oppholdstiden varierer over tid, kan da en gjennomsnittlig, effektiv vanntransport \bar{q}_{inn} over en simuleringstidsperiode som går fra tid T_1 til tid T_2 beregnes ved å integrere denne ligningen over tid:

$$\bar{q}_{inn} = \frac{1}{T_2 - T_1} \int_{T_1}^{T_2} \frac{V}{\tau} \left(1 - \frac{d\tau}{dt} \right) dt = \frac{1}{T_2 - T_1} \left(\int_{T_1}^{T_2} \frac{V}{\tau} dt - \int_{T_1}^{T_2} \frac{V}{\tau} \frac{d\tau}{dt} dt \right)$$

I praksis vil beregningen skje ved å summere over et endelig antall tidskritt; for et slikt tidskritt Δt har vi

$$q_{inn}\Delta t = \frac{1}{2} \left(\frac{V}{\tau} + \frac{V + \Delta V}{\tau + \Delta\tau} \right) (\Delta t - \Delta\tau)$$

Denne ligningen forutsetter at τ er >0 gjennom hele tidsintervallet. Dersom vi starter fra $t=0$ med $\tau=0$, vil vi i startpunktet ha $(d\tau/dt)=1$, og over et lite tidsrom Δt , hvor både V og q_{inn} varierer relativt lite, vil vi da tilnærmet ha:

$$\tau = t - kt^2$$

Med tilnærmet lineær variasjon i volum med tiden gir det:

$$q_{inn} = \frac{2 \left(V + \frac{\Delta V}{\Delta t} t \right) k}{1 - kt}$$

Integralet av q_{inn} blir da:

$$\bar{q}_{inn}\Delta t = 2 \int_0^{\Delta t} \frac{V + \frac{\Delta V}{\Delta t} t}{1 - kt} k dt = -2 \int_1^{1-k\Delta t} \frac{V + \frac{\Delta V}{k\Delta t} (1-u)}{u} du$$

som tilnærmet blir:

$$\bar{q}_{inn}\Delta t = -\ln(1 - k\Delta t) \left(V + \frac{\Delta V}{k\Delta t} \right) - \Delta V$$

Hvis $k\Delta t \ll 1$, gir det tilnærmet:

$$\bar{q}_{inn}\Delta t = \left(V + \frac{\Delta V}{2}\right)k\Delta t = \left(V + \frac{\Delta V}{2}\right)\frac{(\Delta t - \Delta\tau)}{\Delta\tau}$$

En alternativ forenklet betraktning, som teoretisk ikke skulle være så riktig, vil være å beregne gjennomsnittlig oppholdstid, dvs.

$$\bar{\tau} = \frac{1}{T_2 - T_1} \int_{T_1}^{T_2} \tau dt$$

og deretter beregne gjennomsnittlig transport inn ved formelen

$$\bar{q}_{inn} = \frac{V}{\bar{\tau}}$$

Det vil bare være riktig dersom variasjonene i q_{inn} og τ ikke har noen sammenheng, hvilket selvsagt ikke er riktig. For en stasjonær situasjon, hvor både volum og fluks er konstant i tid, vil ligningen imidlertid være riktig.

For tidsvarierende transport eller volum kan transporten ut beregnes av $V(t)$ og q_{inn}

2.2 Oppholdstid i sammensatt volum

Hvis volumet V i stedet for å være velblandet er satt sammen av en serie av N delvolumer v_k ($k=1, \dots, N$), kan den samlede oppholdstiden innenfor volumet V beregnes som

$$\tau(t) = \frac{1}{V} \sum_{k=1}^N v_k \tau(t)_k$$

Oppholdstiden i hvert delvolum beregnes da ved numerisk integrasjon på samme måte som beskrevet ovenfor, men etter en modifisert ligning:

$$\frac{d\tau_k}{dt} = 1 - \frac{1}{v_k} \left(q_{0k} \tau_k + \sum_{r \neq k} q_{rk} (\tau_r - \tau_k) \right)$$

hvor q_{rk} betegner transport fra delvolum r til delvolum k , men q_{0k} betegner transport inn utenfra direkte til delvolum k .

Deretter beregnes den samlede oppholdstiden som middel over alle delvolumene, og så brukes de samme tidsintegralene som beskrevet ovenfor på den samlede oppholdstiden. De beregnede transportene regnes som de effektive transportene inn i volumet mht. oppholdstid, og tilnærmet også for andre konsentrasjoner.

3. Beregning av oppholdstider og effektive transporter ved hjelp av NIVAs fjordmodell

3.1 Skisse av beregningsoppsettet

Oppholdstid innenfor modellvolumet kan i eksisterende modellversjon beregnes ved hjelp av en tilstandsvariabel `CONC1` som primært brukes til å sjekke volumkontinuitet, men også etter valg til å beregne oppholdstid innenfor et volum som består av ett eller flere bassenger. Bruken av variabelen er styrt av et sett av kontroll-variable.

De to funksjonene splittes nå opp, slik at den opprinnelige array-variabel `CONC1` (navnet om fra `C1`) med ett element for hvert lag bare brukes til å sjekke volumbevaring i modellen, som en variabel som skal holde seg =1. (Modellen behandler volum som konservativt, dvs. at den neglisjerer endringer pga. trykk og ikke-lineær respons ved blanding av vann med ulik temperatur og saltholdighet).

Beregning av oppholdstider er flyttet til et ny array `ResidTime(dim_MLI, dim_ResidTime)` slik at en kan ha opptil `dim_ResidTime` ulike definisjoner av volumer hvor en vil se på oppholdstiden. Hvert lag kan tilhøre ett eller flere volumer, eller ligge utenfor alle. Dvs. at det i prinsippet er full fleksibilitet i definisjon av oppholdstids-volumene, selv om en i praksis selvsagt bare vil definere slike volumer som består av sammenhengende sett av vannlag.

`ResidTime(i,k)` angir da hvor lenge vannet innenfor lag nr. i gjennomsnittlig har oppholdt seg innenfor volum nr. k , dersom laget tilhører volumet, hvis ikke holdes verdien på 0.

Underveis i simuleringen oppdateres verdiene slik at `ResidTime(i,k)` for lag i som tilhører volum k øker med 1 pr. tidsenhet. `ResidTime` oppdateres ellers som en vanlig konsentrasjon, dvs. at blanding av vann gir lineær blanding av `ResidTime`. Verdien av `ResidTime` i ulike lag vil da være et direkte mål på oppholdstid innenfor de definerte volumene. Oppholdstid for hele volumet beregnes som et volumvektet middel over modell-lagene, og effektiv innstrømning beregnes av formlene ovenfor for hvert tidsskritt. Både oppholdstid og effektiv innstrømning akkumuleres over tid som tidsintegral, og git grunnlag for å beregne gjennomsnittlig oppholdstid og gjennomsnittlig effektiv innstrømning gjennom simuleringen.

Volumene defineres av bruker ved at det før kjøringene spesifiseres et array `ResTimeZLIMIT(2, dim_MBI, dim_ResidTime)`. Her legges inn dypgrenser for hvert basseng som avgrensner hvilke lag innen bassenget som tilhører hver definisjon av oppholdstid. `ResTimeZLIMIT(k, IB, I_RT)` for $k=1,2$ angir dyp-avgrensning mot henholdsvis overflaten og mot største dyp for basseng `IB`, volumdefinisjon `I_RT`. Alle lag i bassenget med dyp innenfor disse dypgrensene hører til det definerte volumet en vil ha beregnet oppholdstiden innenfor. Lagene tilhører volumet hvis midlere dyp (`ZMID`) ikke ligger dypere enn nedre dyp-grense, og dypere enn øvre dyp-grense. Hvis det som er nedre grense i en volumdefinisjon da er lik øvre grense i en annet volumdefinisjon, vil lag på overgangen bare bli tilordnet en volumdefinisjon.

Ved oppstart av hver kjøring sjekker modellen volumdefinisjonene mot den aktuelle lagdelingen, og setter opp et heltalls-array `ResidVolLayer(2, dim_MBI, dim_ResidTime)`, hvor `ResidVolLayer(i, b, r)` angir hhv. første og siste lag ($i=1,2$) fra basseng b som inngår i volum r .

3.2 Volumdefinisjoner

POP-modellen har 6 delvolumer, som vist i figur 1.

Volumnr	Bunnefjorden	Vestfjorden
0-20 m	1	4
20-50 m	2	5
50-200 m	3	6

Figur 1. Prinsippskisse av volumene i POP-modellen for indre Oslofjord. Bunnefjorden inkluderer Havnebassenget og Bekkelagsbassenget, og Vestfjorden inkluderer Bærumsbassenget.

For å estimere transporter er disse volumene, og også noen kombinasjoner av dem, definert i fjordmodellen for beregning av oppholdstid. De definisjonene som er prøvd brukt, er gitt i tabell 1, med dypgrenser angitt som tallpar *ResTimeZLIMIT(1,..)-ResTimeZLIMIT(2,..)*. For volumdefinisjoner hvor hele bassenget er utenfor, er dette markert med - i tabellen, da settes grensene like, f.eks. 0-0, slik at ingen lag blir med.

Tabell 1. Definisjon av volumer for beregning av oppholdstid i NIVAs fjordmodell

Volum nr	Bunnefjorden (inkludert Bekkelaget og Oslo havn)	Vestfjorden (inkludert Bærumsbassenget)	
1	0-20 m	-	Bare ett delvolum i modellen
2	20-50 m	-	
3	50m-bunn	-	
4	-	0-20 m	
5	-	20-50 m	
6	-	50m-bunn	
7	0m-bunn		Kombinasjon del-volumer innenfor ett basseng
8	20m-bunn		
9	0-50 m		
10		0m-bunn	
11		20m-bunn	
12		0-50 m	
13	0m-bunn	0m-bunn	Hele fjorden
14	20m-bunn	20m-bunn	
15	0-50 m	0-50 m	

Slik fjord-modellens topografi er spesifisert, har den lagtykkelse på ca. 2 m omkring 20 m dyp, med en lag-grense akkurat i 20 m dyp, og lagtykkelse omkring 4.5 m rundt 50 m dyp, med laggrenser i 47.16 og 51.8 m dyp. Det medfører at de faktiske dypene for inndeling av volumer blir 20 m og 51.8 m. Det er ikke noe vesentlig avvik fra de spesifiserte 20 og 50 m dyp.

3.3 Praktisk beregning av oppholdstid og effektiv bruttotransport pr. volum

Det er kjørt en simulering over 14 år. Oppholdstidene øker fra 0 ved starten av simuleringen inntil de når en slags kvasi-likevekt etter ca. 4 år. Da startes akkumuleringen av gjennomsnittsverdier for oppholdstidene, med beregning av midlere oppholdstid ved slutten av simuleringen. Dvs. at midlere oppholdstid for volum i , og midlere effektiv innstrømning beregnes ved hhv.

$$\bar{\tau}_i = \frac{1}{3650} \int_{t=1460}^{t=5110} \tau(t)_i dt \qquad \bar{q}_i = \frac{1}{3650} \int_{t=1460}^{t=5110} q(t)_i dt$$

hvor $\tau(t)_i$ er oppholdstiden i volum i ved tidspunkt t . Oppholdstiden ved et bestemt tidspunkt betyr altså hvor lenge det vannet som er i volum i ved tid t i gjennomsnitt har oppholdt seg innenfor volumet. Resultatene er oppsummert i tabell 2.

Tabell 2. Resultater fra simulering med NIVAs fjordmodell for volumene definert i tabell 1. Bf: Bunnefjorden, Vf: Vestfjorden

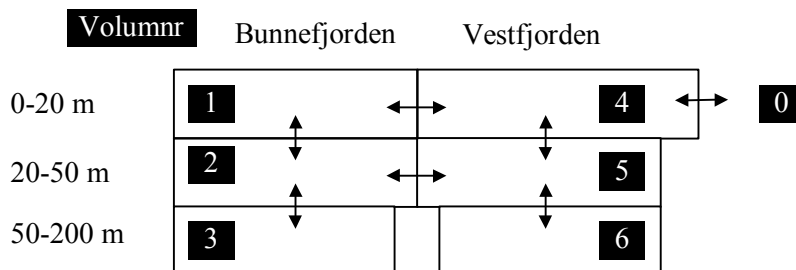
A	B		C	D	E	F
Volum nr. (i)	Volumdefinisjon		Volum V_i mill. m ³	$\bar{q}_i = \frac{1}{3650} \int_{t=1460}^{t=5110} q(t)_i dt$ m ³ /s	$\bar{\tau}_i = \frac{1}{3650} \int_{t=1460}^{t=5110} \tau(t)_i dt$ dager	$\bar{q}_i = \frac{V_i}{\bar{\tau}_i}$ m ³ /s
1	Bf	0-20 m	1018	885	14.4	818
2	Bf	20-50 m	1058	372	36	340
3	Bf	50m-bunn	976	597	210	54
4	Vf	0-20 m	2379	2009	14.5	1896
5	Vf	20-50 m	2382	890	34	806
6	Vf	50m-bunn	1524	212	103	171
7	Bf	0m-bunn	3052	171	222.5	159
8	Bf	20m-bunn	2034	84.0	312	75
9	Bf	0-50 m	2077	712.5	35	690
10	Vf	0m-bunn	6285	763	98	739
11	Vf	20m-bunn	3906	384	126	359
12	Vf	0-50 m	4761	1542	36	1512
13	Bf+Vf	0m-bunn	9337	464	234	461
14	Bf+Vf	20m-bunn	5939	271	261	264
15	Bf+Vf	0-50 m	6838	1078	75.2	1052

Egentlig burde en vente at direkte beregning av effektiv innstrømning i kolonne D skulle gi bedre resultat enn å bruke midlere oppholdstid (kolonne E,F). Resultatene viser imidlertid at for volumene under 50 m, volum 3 og 6, gir den direkte beregningen i kolonne D et helt urimelig forhold mellom transportene for Bunnefjorden og Vestfjorden, med nesten tre ganger så stor utveksling i Bunnefjorden som i Vestfjorden. Det står i sterk kontrast fjordmodellens forutsetninger, basert på analyse av data, om at dypvannet i Bunnefjorden har mye mindre vertikalblanding og sjeldnere dypvannsfornyelser enn

Vestfjorden. Vestfjorden har vertikalblanding pga. dissipering av interne bølger generert ved Drøbaksterskelen, som ikke gjør seg gjeldende på samme måte i Bunnefjorden, og derfor ca. 5 ganger sterkere vertikalblanding. Midlere oppholdstid i kolonne *E* stemmer bedre med en slik antagelse, og de transporter som anslås ut fra oppholdstidene har også et rimelig forhold, nemlig ca. 3 ganger større utveksling i Vestfjorden som absolutt-tall¹. Det fremgår av tabellen at det er volumet av Bunnefjorden under 50 m som får en urimelig høy transportverdi i kolonne *D*. For de andre volumene gir kolonne *D* og *F* omtrent samme resultat. Konklusjonen blir at det beste er å basere anslagene for volumtransporter på den formelt mindre riktige beregningen ut fra midlere oppholdstid for alle volumene, dvs. kolonne *F*.

3.4 Beregning av transporter i grenseflater mellom volumene

Målet er å anslå effektive transporter over grenseflatene mellom volumene. Med den oppdeling som er valgt i POP-modellen, blir det 7 toveis transporter som skal beregnes, eller 14 enveis transport-tall, som vist i skissen nedenfor. Transporten fra volum *i* til volum *k* betegnes med $q_{i,k}$.



Lokale ferskvannstilførsler er relativt uvesentlige, men kan evt. legges inn med 10 m³/s inn til hvert av overflatevolumene, med notasjon f_1 og f_4 . Ferskvann gjennom renseanleggene er neglisjerbare i forhold til de beregnede transportene. Overflatelaget består av brakkvann, dvs. en blanding av ferskvann og sjøvann. Uansett om denne innblanding skjer ved horisontal utveksling pga. tidevann og vinddrevne bevegelser eller ved innblanding av vann nedenfra (estuarin-sirkulasjon), vil det skje innenfor det øverste modell-laget fra 0 til 20 m, og i POP-modellen vil det derfor bare inngå som horisontal utveksling i de øverste volumene.

Til å bestemme de 14 ukjente transportene har vi i utgangspunktet de beregnede brutto fluksene inn i de forskjellige definerte volumene. Med estimater for totale volumfluks QB_j inn i hvert av de definerte volumene som beskrevet i kapittel 0, burde det, hvis alle volumene var velblandede, kunne settes opp et lineært ligningssystem som kan løses for å beregne enkelttransporter. For eksempel burde brutto innstrømning QB_1 til volum 1 være gitt ved ligningen

$$QB_1 = f_1 + q_{2,1} + q_{4,1}$$

altså ved summen av innstrømning fra volum 2 og 4, i tillegg til ferskvannstilførselen. Av de 15 definerte delvolumene fås 15 slike betingelser. I tillegg er det en del kontinuitetsbetingelser som kunne brukes. Alle ligningene er ikke uavhengige, men det er likevel i prinsippet mer enn nok ligninger til å bestemme de ukjente. Ved å ha like mange ligninger som ukjente skulle en i prinsippet finne en entydig løsning. Imidlertid er

¹ De to forholdstallene er ikke direkte sammenlignbare. Vertikalblanding er pr. areal, mens transportene er beregnet som absolutte tall. Forholdstallet for vertikalblanding gjelder dessuten bare turbulent blanding mellom dypvannsfornyelser, mens selve dypvannsfornyelsen også vil inngå i transport-tallet.

modellvolumene som nevnt ikke velblandede, og da kan en ikke vente at ligningene skal gå opp. Et forsøk på å finne en løsning på denne måten har ikke ført frem; ulike ligninger kan gi motstridende betingelser, og en kan også få negative transporter. Selv en løsning hvor en opererer med flere ligninger enn ukjente, og finner en løsning ved å minimere kvadrat-avvik, fører ikke frem til en fornuftig løsning.

Det er derfor brukt en enklere fremgangsmåte, hvor de transportene som er beregnet i kolonne F i tabell 2 anvendes mer uformelt til å sette opp et transportbilde mellom volumene.

Det er naturlig å ta utgangspunkt i de to volumene under 50 m dyp. Krav til volumkontinuitet tilsier nettotransport 0 inn i disse volumene, dvs. at det skjer en vertikal utveksling mellom volum 2 og 3 og mellom 5 og 6, med like transport-tall begge veier.

Det gir:

$$q_{2,3} = q_{3,2} = QB_3 = 54 \text{ m}^3/\text{s}$$

$$q_{5,6} = q_{6,5} = QB_6 = 171 \text{ m}^3/\text{s}$$

Tilsvarende har vi for volum 13, som er hele fjordvolumet innenfor Drøbak, en sammenheng:

$$q_{4,0} = q_{0,4} + f_1 + f_4 = QB_{13} = 461 \text{ m}^3/\text{s}$$

og med ferskvannstilførsler f_1 og f_4 som begge er $10 \text{ m}^3/\text{s}$ gir det

$$q_{4,0} = 461 \text{ m}^3/\text{s}$$

$$q_{0,4} = 441 \text{ m}^3/\text{s}$$

For de andre 4 interne grenseflatene er ikke nødvendigvis transportene like i begge retninger. Generelt kunne en tenke seg å beskrive transportene som et sett utvekslinger av diffusiv karakter, med lik transport i begge retninger, overlappet en netto rotasjon $1 \rightarrow 4 \rightarrow 5 \rightarrow 2 \rightarrow 1$. Vi har imidlertid ikke noe godt grunnlag for å anslå forskjeller noen kontinuitetsbetingelser, og det mest naturlige er å anta at transportene er like i begge retninger over hver grenseflate, men unntak av grenseflaten mellom volum 1 og 4, hvor ferskvannstilførselen til volum 1 kommer inn som en korleksjon. Dette gir følgende betingelser:

$$q_{1,2} = q_{2,1}$$

$$q_{4,5} = q_{5,4}$$

$$q_{1,4} = q_{4,1} + f_1$$

$$q_{2,5} = q_{5,2}$$

For å knyttet enkelttransporter til brutto inntransport er det mest naturlige å se på de 4 øverste enkeltvolumene. Vi kan da sette opp disse sammenhengene:

$$q_{21} + q_{4,1} + f_1 = QB_1$$

$$q_{1,2} + q_{3,2} + q_{5,2} = QB_2$$

$$q_{1,4} + q_{5,4} + q_{0,4} + f_2 = QB_4$$

$$q_{2,5} + q_{4,5} + q_{5,6} = QB_5$$

Vi kan nå eliminere ukjente ved hjelp av betingelsene ovenfor, og flytte alle kjente og allerede estimerte størrelser over på høyre side i ligningene. Det gir følgende 4 ligninger med 4 ukjente:

$$q_{1,2} + q_{1,4} = QB_1$$

$$q_{1,2} + q_{2,5} = QB_2 - q_{3,2}$$

$$q_{1,4} + q_{4,5} = QB_4 - q_{0,4} - f_2$$

$$q_{2,5} + q_{4,5} = QB_5 - q_{5,6}$$

Ved å sette inn tallverdier og skrive ligningen på matrisform har vi:

$$\begin{bmatrix} 1 & 1 & 0 & 0 \\ 1 & 0 & 1 & 0 \\ 0 & 1 & 0 & 1 \\ 0 & 0 & 1 & 1 \end{bmatrix} \times \begin{bmatrix} q_{1,2} \\ q_{1,4} \\ q_{2,5} \\ q_{4,5} \end{bmatrix} = \begin{bmatrix} 818 \\ 286 \\ 1445 \\ 635 \end{bmatrix}$$

Det gir likevel ikke direkte noen løsning, fordi ligningene er selvmotsigende². Det ses lett ved å kombinere hhv. ligning (1, 3) og (2,4), som gir hhv.

$$q_{1,2} - q_{4,5} = 818 - 1445 = -627$$

$$q_{1,2} - q_{4,5} = 286 - 635 = -349$$

En kunne selvsagt prøve å velge ut kombinasjoner av volumer som gir fornuftige resulater, men det blir uansett nokså tilfeldig. I stedet velger vi å fortsette å se på betingelsene for de 4 enkeltvolumene, men bruker dem bare til å anslå transporter av noenlunde riktig størrelsesorden, uten å krevne en eksakt øsning av ligningene. Ut fra de to motstridende ligningene ovenfor kan vi f.eks. anslå at $q_{4,5}$ er ca. 450-500 m³/s større enn $q_{1,2}$. Vi prioriterer å få transporter som gir volumkontinuitet. Som retningslinje velger vi å sette de to vertikale transportene $q_{1,2}$ og $q_{4,5}$ slik at forholdet mellom dem blir noenlunde som forholdet mellom de dypereleggende transportene $q_{2,3}$ og $q_{5,6}$. Etter litt manuelle justeringer velges følgende transporttall:

$$q_{1,2} = 150 \text{ m}^3/\text{s}$$

$$q_{4,5} = 500 \text{ m}^3/\text{s}$$

$$q_{1,4} = 600 \text{ m}^3/\text{s}$$

$$q_{2,5} = 135 \text{ m}^3/\text{s}$$

Når dette settes inn i de fire betingelsene, fås:

$$q_{1,2} + q_{1,4} = 850 \text{ m}^3/\text{s} \quad (\text{ønsket verdi } 818 \text{ m}^3/\text{s})$$

$$q_{1,2} + q_{2,5} = 285 \text{ m}^3/\text{s} \quad (\text{ønsket verdi } 286 \text{ m}^3/\text{s})$$

$$q_{1,4} + q_{4,5} = 1250 \text{ m}^3/\text{s} \quad (\text{ønsket verdi } 1450 \text{ m}^3/\text{s})$$

$$q_{2,5} + q_{4,5} = 635 \text{ m}^3/\text{s} \quad (\text{ønsket verdi } 635 \text{ m}^3/\text{s})$$

Disse transportverdiene har altså både noenlunde rimelig verdier ut fra en skjønnsmessig vurdering, og tilfredsstillende betingelsene som følger av modellsimuleringsresultatene relativt godt, iallfall med nokså små relative avvik for brutto-transporter og oppholdstider.

² Matematisk: Koeffisientmatrisen har determinant =0, mens den matrisen en får ved å sette inn vektoren på høyre side i en av radene får determinant ≠0.

For å oppsummere, med litt avrundede verdier:

$$q_{1,2} = q_{2,1} = 150 \text{ m}^3/\text{s}$$

$$q_{2,3} = q_{3,2} = 55 \text{ m}^3/\text{s}$$

$$q_{4,5} = q_{5,4} = 500 \text{ m}^3/\text{s}$$

$$q_{5,6} = q_{6,5} = 170 \text{ m}^3/\text{s}$$

$$q_{2,5} = q_{5,2} = 135 \text{ m}^3/\text{s}$$

$$q_{1,4} = 600 \text{ m}^3/\text{s}$$

$$q_{4,1} = q_{1,4} - f_1 [= 590 \text{ m}^3/\text{s}]$$

$$q_{4,0} = 460 \text{ m}^3/\text{s}$$

$$q_{0,4} = q_{4,0} - (f_1 + f_2) [= 440 \text{ m}^3/\text{s}]$$



Norwegian Institute for Air Research (NILU)

P.O. Box 100, N-2027 Kjeller, Norway

REPORT SERIES SCIENTIFIC REPORT	REPORT NO. OR 24/2003	ISBN 82-425-1444-5 ISSN 0807-7207	
DATE	SIGN.	NO. OF PAGES 48	PRICE NOK 150,-
TITLE The Oslofjord POP Model v. 1.0 A Fugacity-Based Non-Steady State Non-Equilibrium Multimedia Fate and Transport Model		PROJECT LEADER Knut Breivik	
		NILU PROJECT NO. N-100159	
AUTHOR(S) Knut Breivik ¹ , Birger Bjerkgeng ² , Frank Wania ³ , Jan Magnusson ² , Aud Helland ² and Jozef M. Pacyna ¹		CLASSIFICATION * A	
		CONTRACT REF. Knut Breivik	
REPORT PREPARED FOR Norges Forskningsråd Postboks 2700 St. Hanshaugen 0131 OSLO			
ABSTRACT This report describes in detail the development and parameterisation of the Oslofjord POP Model – a fugacity based mass balance model developed to understand and predict the fate of POPs in the Oslofjord, Norway. The model has been developed as part of a research project, entitled “Development and evaluation of a model strategy for POPs in contaminated fjord areas - a case study for PCBs in the Oslofjord” (NFR-project No. 140530/720). The model calculates the environmental distribution, transport and fate of POPs, based on information about environmental characteristics, physical-chemical properties and half-lives as well as historical emissions and advective inflows.			
NORWEGIAN TITLE Oslofjord POP modellen versjon 1.0 En dynamisk massebalansmodell som beskriver skjebnen til organiske miljøgifter i Oslofjorden.			
KEYWORDS Multimedia fate model	POPs	Oslofjorden	
ABSTRACT (in Norwegian) Denne rapporten beskriver i detalj en dynamisk fugasitetsbasert multimedia modell som er utviklet for å forstå og forutsi transport og omsetningsforhold for organiske miljøgifter i Oslofjorden. Modellen som er beskrevet er utviklet som del forskningsprosjektet ”Utvikling og evaluering av en modell-strategi for organiske miljøgifter i belastede fjordområder – en studie av PCB i Oslofjorden” finansiert av forskningsrådet (NFR, prosjektnummer 1405320/720). Modellen kan benyttes på de fleste PC'er av nyere dato og kan fås tilgang til gratis ved å kontakte NILU.			

* Classification A Unclassified (can be ordered from NILU)
 B Restricted distribution
 C Classified (not to be distributed)